**Response to Reviewers**

We thank the reviewers for their constructive and helpful suggestions. We have provided our responses to the reviewers' comments and believe that our manuscript is much improved as a result.

The main paper improvements are:

- The abstract was rewritten.
- The goal of the study is formulated more clearly.
- The number of sites for validation of GELCA is increased.
- Proofreading and grammar check performed.

The reviewer's specific comments (shown in blue) are addressed below.

## Response to Anonymous Referee #1

Received and published: 8 September 2015#1:

The manuscript by Belikov et al. presents the development of a new adjoint modeling system A-GELCA. The novelty of this tool is combining a Lagrangian back trajectory model with an Eulerian adjoint model. The authors provide background on issues related to inverse modeling of CO2, which seems to be the intended application of this tool. The model estimates for various configurations (different resolutions of the Eulerian component) are shown compared to CO2 measurements from seven stations in Siberia. This is followed by evaluation of the model via comparison to forward modeling sensitivities and the Lagrange equality. Lastly, the authors show comparisons of adjoint sensitivities for different model configurations, highlighting the information brought through the coupling of Lagrangian and Eulerian components. The tools presented here seem to perform adequately and will be of value for future application studies. My main criticism is a lack of detail in many places in the manuscript, particularly when covering some of the more essential and novel aspects of the model development (how the Eulerian and Lagrangian components were coupled, or how the adjoint code was developed). Further, the article needs much work on the grammar and writing. I believe it will be suitable for publication after addressing these and other issues outlined below.

Comments:

Scope: It seems like evaluation of the forward model is a substantial part of this work; as such, this should be included in the abstract and introduction as one of the aims of the article, and the title itself should reflect this scope.

The goal of this study is to present the development and evaluation of an Adjoint of the Global Eulerian–Lagrangian Coupled Atmospheric model (A-GELCA). Evaluation of the forward model is necessary to show the potential of the proposed method.

Abstract and throughout: it seems odd to refer to "development of the adjoint of a Lagrangian model", since Lagrangian models are self adjoint by construction. So saying "Lagrangian adjoint" seems redundant.

Text in the paper was revised. "Lagrangian adjoint" is replaced with "Lagrangian component"

5984.17: this entire sentence is rather vague. Could the authors clarify, quantitatively, what is mean by "effective in reproducing", "high uncertainty" and "low resolution"? Without any numbers, such statements have little context or impact.

The sentence revised as follows: “The forward simulation shows that the coupled model improves reproducing of the seasonal cycle and short-term variability of $CO_2$.”

However, we do not consider it is necessary to include any numbers in the introduction. More details were added to main part.

5985.13: Can the authors be any more specific than “a number of studies have proposed improvements” and then citing several papers? What are the improvements, and which are relevant to the topic of this work in terms of those related to resolution, or coupled Eulerian/Lagrangian frameworks?

Revised as follows:

“A number of studies have proposed improvements to the inverse methods of atmospheric transport, i.e. the efficient computation of the transport matrix by the model adjoint proposed by Kaminski et al. (1999b), use of monthly mean GLOBALVIEW-$CO_2$ ground-based data (current version is for 2014) by Rödenbeck et al. (2003), development an ensemble data assimilation method by Peters et al. (2005), flux inversion at high temporal (daily) and spatial (model grid) resolution using for the first time of continuous $CO_2$ measurements over Europe by Peylin et al. (2005), use satellite data to constrain the inversion of $CO_2$ by Chevallier et al. (2005), develop of a new observational screening technique by Maki et al. (2010).”

Paper by Kaminski et al. (1999b) is related to the adjoint. Paper by Chevallier et al. (2005) is related to use of satellite data. Flux inversion at high temporal (daily) and spatial (model grid) resolution using for the first time of continuous $CO_2$ measurements over Europe is discussed by Peylin et al. (2005).

Eulerian/Lagrangian frameworks is discussed later (5987.10-16): “In order to exploit the advantages of both methods, Lagrangian and Eulerian chemical transport models can be coupled to develop an adjoint, that is suitable for the simultaneous estimation of global and regional emissions. Coupling can be performed in several ways; e.g., a regional-scale LPDM can be coupled to a global Eulerian model at the domain boundary (Rödenbeck et al., 2009; Rigby et al., 2011), or a global-scale LPDM can be coupled to an Eulerian model at the time boundary (Koyama et al., 2011; Thompson and Stohl, 2014).”

5985.20: For recent measurement updates, a reference from 1999 doesn’t seem very recent.

Replaced with (Karion et al., 2013; Tohjima et al., 2015)

5986.16: It would take a prohibitively large number of forward model evaluations to evaluate such a matrix for an inversion with the same resolution of an adjoint-based approach.

Revised as: "Theoretically, to compute such matrix the transport model is run multiple times with set of prescribed surface fluxes. However, this would require an extremely large number of forward model evaluations. The adjoint of the transport model is an efficient way to accelerate calculation of concentration gradient of the simulated tracer at observational locations (Kaminski et al., 1999)."

5986.24: "Recent studies. . ." It seems odd to switch the discussion here to CO, given the previous focus on long-lived tracers, CO2 in particular. Why not instead cite/discuss the set of current studies using adjoint models to invert satellite CO2 data? I believe there are several.

Revised as follows: "Recent studies have used this method to constrain estimates of the emissions of $CO_2$ using retrieved column integrals from the GOSAT satellite (Basu et al., 2013; Deng et al., 2014; Liu et al., 2015)."

5986.28: ". . .speeds the process of inverse modeling" is only true for high dimensional systems.

In 5985.23-30 we stated: "The satellite observation data from current (GOSAT, Kuze et al., 2009; Yokota et al., 2009; OCO-2, Crisp et al., 2004) and future missions (CarbonSat/CarbonSat Constellation; Bovensmann et al., 2010; Buchwitz et al., 2013) offer enormous potential for $CO_2$ inverse modeling. Optimal application of large observed datasets requires expanding the inverse analysis of $CO_2$ to finer resolution, higher precision and faster performance." A large number of observations and resolution of the considered model indicate that the existing and developing inverse modeling system can be attributed to the high dimensional systems.

5988.20: The background. . ." I didn't really understand what was being said here or how the modeling setup works in this regards.

Here "The background grid values of the concentrations" are the concentrations calculated by Eulerian model.

To clarify the sentences about the model setup we revised section 2.1.

5989.3: The description of the coupling of the eulerian adjoint model with the Lagrangian model is rather vague. This statement, that it was coupled at the "time boundary" is made a few times, but to be honest I don't really know what it means. Given that (a) this coupling is the single most unique and exciting feature of the A-GELCA model and (b) articles in GMD are for the expressed purpose of describing algorithmic model details, this should clarified in further detail, at the level of making the process understandable and reproducible by a reader.

We revised section 2.1 and added short descriptions of coupling procedure to the text to clarify the sentences about the time boundary coupling: "The scheme of concentration calculation for the given location includes coupling of two model approaches. NIES TM calculates global concentrations for the selected time period (usually 1 year to exclude spin-up effect), but stops 7 days before the time of the observations. To obtain the concentrations for the observation time we transport the background concentrations from NIES TM gridbox to the location of observation point along the trajectory ensemble calculated by FLEXPART model and add contribution from surface sources. Therefore we have implemented the coupling at a time boundary in the global domain of the NIES transport model, while nested regional modeling systems such as one by Rodenbeck et al (2009) have to couple at both region boundary and time boundary."

Here we just repeat the main features of the coupling. Detailed information may be found in original paper by Ganshin et al. (2012).

5989.25: "performs well" is very vague. Can the authors be more specific?

The text is revised as follows: "To ensure that this is the case, the NIES TM model has been evaluated extensively. Comparisons against $SF_6$ and $CO_2$ (Belikov et al., 2011, 2013b), $CH_4$ (Patra et al., 2011; Belikov et al., 2013b), and $^{222}Rn$ (Belikov et al., 2013a) measurements show the model ability to reproduce seasonal variations, interhemispheric gradient and vertical profiles of tracers." For details please check papers shown above.

5992.5: Is it that the errors are unbiased or that the background estimate itself is unbiased?

Here it is assumed, the model simulations are unbiased. Observations are unbiased normally.

5992.6: This capital bold H applied as a matrix is already linear by definition. If the authors intended to more generally describe a potentially nonlinear forward model operator, they should use capital cursive H.

Revised as follows: “The minimization of the cost function (Eq. 2) has an analytic solution …”

Did the authors also generate/evaluate a tangent linear model? If not, what is there intended path towards deriving an inverse modeling system (many formulations of which require a tangent linear model, i.e., incremental 4D-Var with CG optimization, etc)? Or will their system only worth with optimization approaches such as using the BFGS variable-metric quasi-newton algorithm?

Yes, we constructed tangent linear model. We stated “The tangent linear and adjoint components of the Eulerian model …” at 5984.7, 5994.1, 5999.22.

5993.11: Previously (5992.24) a 1x1 scale was referred to as low resolution, but here 1x1 is used for the “high resolution” FLEXPART runs. This is a bit inconsistent. I was expecting FLEXPART simulations to be run at a much finer (i.e. 10’s of km) scale.

At line 5992.24 the sentence “standard low-resolution” replaced with “standard resolution”.

Currently we have no meteorological data suitable to run the FLEXPART model with higher resolution (i.e. 0.5 degree). However, use a model with resolution of 1x1 degree for flux inversion is normal now.

The set of measurements used for evaluation (7 sites) seems pretty thin compared to the amount of available CO2 measurements available. The NOAA GMD network alone has more than 100 measurement sites. Now, perhaps forward model evaluation isn’t a goal of this work (see previous discussion, this wasn’t clear), but if it is then it should be done more comprehensively.

Number of sites for validation of GELCA is increased. Section 4 was revised.

5994.7: “We recognize. . . is quite problematic” I didn’t understand the point that the authors are trying to make here. Can they reword?

Reworded: “We recognize that is quite problematic to use the highly uncertain surface fluxes to simulate the tracer concentrations and use these concentrations for estimating the quality of different model configurations. Nevertheless, we cannot improve our analysis, because we do not have concentration measurements for tracers whose surface fluxes are more accurately known, like SF6.”

5994.22: I recognize that there are continuous vs discrete approaches for developing adjoint models, that there are benefits/drawbacks to each approach, and that the authors have adopted the discrete approach for specific reasons. But is it fair to only here mention the benefits of this approach, and none of the drawbacks?

We added "The main drawback of the method is that the deriving of discrete adjoint of Eulerian model is a significant technical challenge."

5996: For the forward model sensitivity, use lambda_F throughout, not just in equation 5.

Revised accordantly.

5996.14: Why is a perturbation needed for an adjoint simulation? Do you mean forcing? Or that the cost function was defined to be 1 ppm per grid cell?

There was misprint in this section.

The text was revised, as: "In the first test, adjoint simulations were carried out using an initial $CO_2$ distribution, zero surface flux for 2 days (1-2 January 2010) and a horizontal grid with resolution 2.5° × 2.5°. The adjoint gradient was then compared with that from the finite difference calculated using Eq. (3). This equation was selected in order to save CPU time by minimizing the number of forward model function calculations. For this test we used $\varepsilon = 0.01$."

Section 3: I recognize that the long-term goal is inverse modeling. However, the application and testing of the model thus far is just for sensitivity calculations. It seems then that Section 3 would be better served as a description of adjoint modeling, and the background of how this works, rather than or in addition to inverse modeling, as the latter isn't actually done in the present manuscript. This would help clarify, for example, the setup of the adjoint calculations that are performed later for validation in 5.2.1, which I don't believe used a cost function of the type shown here, but rather something different.

Section 3 is necessary to show why the adjoint has been developed and attach consistency to the article. A simplified form of the described cost function is used to validate the adjoint.

5996.15: The forward sensitivity calculation was performed in how many locations? It seems from Fig 3 that they were done in many grid cells, in order to compare to the adjoint results throughout the domain of this figure, but that would be very expensive, computationally, even using Eq 3. If transport was turned off for the testing, all locations

could have been tested simultaneously, but this wouldn't constitute a very meaningful test of the adjoint of the tracer transport model.

The forward sensitivity calculation was performed using Eq 3 at the same grid cells as for the adjoint simulation. Indeed it is very expensive, computationally. However, this is very powerful test, as it make possible to compare to the adjoint results throughout the domain.

5.2.1: What was the state vector used for these tests? CO2 initial conditions? Fluxes? Or flux scaling factors? What are the corresponding units of the results shown in Fig 3?

The state vector is flux, the target value is concentration. $CO_2$ initial conditions and fluxes are same as for the GELCA forward simulations (added to text). The units (ppm/(μmol/m$^2$s)) are added to the figure caption.

5997.10: It would probably be good to show results from these tests somehow.

We revised text as follows: "We use Eq. (7) to test the adjoint model initialized using several different random random vectors **u** and **v**. For all cases, Eq. (7) compares well within machine epsilon with mismatch between -3e$^{-14}$ to 6e$^{-14}$."

Figs 4-6: These are really interesting results. I found myself, however, having to flip back and forth between these figures to compare across the different modeling approaches. Comparison for a single method across days was much less interesting or relevant to this work. So I would suggest reducing these figures to a single figure that shows the results for a single day but for the 4 methods: eulerian, Lagrangian (native), Lagrangian (aggregated), coupled.

We tried to make the figures easier to compare and combine them appropriately. Section 5.2.2 was revised.

5999: "substantial amount of manual programming effort is required" This should be expanded for a GMD article.

We revised paragraph 5995.1-5 to add more detail about manual code developing, as follows: "The tangent linear and adjoint models of the NIES TM to FLEXPART coupler were derived using the automatic differentiation software TAF (http://www.FastOpt.com), which significantly accelerated the development. However, considerable manual processing of forward and adjoint model codes was necessary to improve the transparency and clarity of the model and to optimize the computational performance of, including MPI, as the TAF code used here (version 1.5) does not fully support MPI routines."

Editorial:

This manuscript needs a thorough proofreading and grammar check prior to publication. I've provided comments below on the abstract and introduction but stopped after that point.

5984.7 tangent –> tangent linear

Revised

5984.6: paragraph break not needed

Revised

5984.11: as results –> as a result

Revised

5984.11: of Eulerian –> of the Eulerian

Revised

5984.17: "test experiments" is redundant, suggest just "tests" or "experiments".

Revised

5984.17: shown –> shows

Revised

abstract: the written tense keeps changing, please try to use a single tense throughout.

The abstract was rewritten.

5984.20: demonstrates the –> is (or was, depending on if you decide to write in the past or present tense throughout) shows to have

5985.18: a density –>the density

Revised

5985.19: measurements –> more measurements

Revised

5985.21: global scale CO2 observation are not existing–> global scale in situ CO2 observations do not exist

Revised

5986.10 CO2 a –> CO2, a

Revised

5986.12: If tracer is a chemically inert –> For chemically inert tracers,

Revised

5986.15: running multiple times with set –> run multiple times with different sets of

Revised

5986.19: Seems odd to have the paragraph break here, instead of e.g. line 22.

Revised

5986.29: “memory demands” should be minimal for adjoint approaches with inert tracer transport (i.e. linear) models.

Indeed, the adjoint approach has relatively low CPU and memory demands. However, here we pointed out computational cost of Eulerian chemical transport models (CTMs) with the high-resolution grids in adjoint and forward simulations.

5987.1 “It would. . ..fluxes” This sentence doesn’t make much sense, and needs to be rewritten.

Revised as follows: “It would be beneficial to increase the model resolution close to observation points, where the strong observation constraint can significantly improve the optimization of the resulting emission fluxes.”

5987.10: utilize of the –> utilize the

Revised

5987.11: the adjoint, which –> an adjoint that

Revised

5987.17: “One goal” is there another goal of this work? Forward model evaluation perhaps? If so this other goal should also be directly stated. If not, suggest saying “The goal”.

Revised. “The goal of this study is …”

Eq 1: why does the “l” index start at 0 and the others at 1?

“l” is a time index, while others are coordinates

## Response to Anonymous Referee #2

Received and published: 8 September 2015

Overview:

The manuscript "Adjoint of the Global Eulerian–Lagrangian Coupled Atmospheric transport model (A-GELCA v1.0): development and validation" by Belikov et al. describes the construction of a new coupled adjoint model based on GELCA, which is a coupled forward transport model based on the NIES Eulerian transport model and the Lagrangian transport model, FLEXPART. The methodology described in this manuscript provides an interesting development upon existing adjoint models, and may be used in future to supply high-resolution adjoint sensitivities at relatively low computational cost. The authors describe the applications of the model, before describing its development and providing examples of the adjoint model's accuracy in comparison with the forward model. Finally, a real-world example of use of the adjoint model is described.

Overall the manuscript is fairly clearly written, although there are a large number of technical corrections necessary before publication. Some of the descriptive sections are quite brief and lacking in necessary detail. The figures and tables are generally clear and well chosen. Although the performance of the forward coupled model compared with the Eulerian model is investigated to some extent, my biggest concern with the manuscript is that only a handful of sites are included in this analysis, all of which are in relatively close proximity to each other, in a region where surface fluxes are uncertain. However, from this limited perspective, the coupling does appear to improve the model performance. The adjoint model is shown satisfactorily to be accurate in comparison with the forward model, which is the most important aspect of the manuscript.

I recommend publication after these revisions have been carried out.

Comments:

5985.11: define 3-D for first use

Done

5985.20: Can you provide a more recent reference than Bovensmann et al., (1999) for this statement?

Replaced with (Karion et al., 2013; Tohjima et al., 2015)

2986.2-4: Rephrase: "Generally, there are the Eulerian and the Lagrangian method of modelling the atmospheric constituents transport"

Rewritten as "Generally, the atmospheric constituents transport may be described in two different ways: the Lagrangian and the Eulerian approaches."

5986.16: Rephrase the sentence beginning “The adjoint of the transport model. . .” as it is unclear.

Revised as: “The adjoint of the transport model is an efficient way to accelerate calculation of concentration gradient of the simulated tracer at observational locations (Kaminski et al., 1999).”

5986.24: The accompanying references to this sentence seem out of place here, as they relate to inverse modelling of CO and NOx, rather than the longer-lived species discussed in the rest of the manuscript.

Revised as follows: “Recent studies have used this method to constrain estimates of the emissions of $CO_2$ using retrieved column integrals from the GOSAT satellite (Basu et al., 2013; Deng et al., 2014; Liu et al., 2015).”

5987.3: You should mention recent work that has made use of nested grids together with inverse modelling methods in order to obtain high-resolution inverse results, such as Hooghiemstra et al., (2012).

Paper by Hooghiemstra et al., (2012) relates “to inverse modelling of CO, rather than the longer-lived species discussed in the rest of the manuscript.” Please see previous comment.

5988.19: Have you investigated the effect of changing the number of particles used in the Lagrangian model (both in terms of information content and computational time)? Perhaps you should mention how you settled on 1000 particles.

Added: “The number of particles has been chosen to optimize the computational cost without compromising the quality of modeling by Ganshin et al., (2013).”

More details are in paper by Ganshin et al., (2013): “One thousand particles were used in the calculations with our method, and this number was found to be optimal by comparing calculations using different numbers of particles. Increasing the number of particles by an order of magnitude (up to 10000) improves the results slightly but increases the required computer time many times. On the other hand, decreasing the number of particles to below 100 markedly worsens model data.”

5989.3: You should clarify what it means to have a coupling at the time boundary in the global domain, rather than at the spatial boundaries. I felt that this was unclear, and should be clearly explained in a development manuscript such as this one.

We revised section 2.1 and added short descriptions of coupling procedure to the text to clarify the sentences about the time boundary coupling: “The scheme of concentration calculation for the given location includes coupling of two model approaches. NIES TM calculates global concentrations for the selected time period (usually 1 year to exclude spin-up effect), but stops 7 days before the time of the observations. To obtain the concentrations for the observation time we transport the background concentrations from NIES TM gridbox to the location of observation point along the trajectory ensemble calculated by FLEXPART model and add contribution from surface sources. Therefore we have implemented the coupling at a time boundary in the global domain of the NIES transport model, while nested regional modeling systems such as one by Rodenbeck et al (2009) have to couple at both region boundary and time boundary.”

Detailed information may be found in original paper by Ganshin et al. (2012).

5989.25: You say that the model performs well in comparison with measurements, but you should further clarify this statement. Can you quantify the performance? Are there any major discrepancies in the model performance in (e.g.) interhemispheric exchange time or vertical mixing?

The text is revised as follows: “To ensure that this is the case, the NIES TM model has been evaluated extensively. Comparisons against $SF_6$ and $CO_2$ (Belikov et al., 2011, 2013b), $CH_4$ (Patra et al., 2011; Belikov et al., 2013b), and $^{222}Rn$ (Belikov et al., 2013a) measurements show the model ability to reproduce seasonal variations, interhemispheric gradient and vertical profiles of tracers." More details are in papers shown above.

5992.6: H is, by definition, already linear if it is a matrix.

Revised as follows: “The minimization of the cost function (Eq. 2) has an analytic solution …”

5993.27-29: I do not think that this statement is supported by the values provided in Table 3. The high-resolution Eulerian model variously outperforms and is outperformed by the low-resolution coupled model at different sites. You should either remove or add qualifications to this line.

Section 4 was revised entirely.

5994.10: Although you have mentioned this in the text, I’m bothered by the fact that you have assessed the model performance at only a few sites in one region of the globe. There

exist a number of observational datasets available for comparisons to model data, such as those provided by the Global Monitoring Division of the National Oceanic and Atmospheric Administration. Can you examine the coupled model performance in tropical regions, for example?

Number of sites for validation of GELCA is increased. Section 4 was revised.

5996.12: This explanation of the model set-up for the accuracy test is a little unclear and should go into more detail. What do you mean by "perturbed by 1ppm per grid cell"?

There was misprint in this section.

The text was revised, as: "In the first test, adjoint simulations were carried out using an initial $CO_2$ distribution, zero surface flux for 2 days (1-2 January 2010) and a horizontal grid with resolution 2.5° × 2.5°. The adjoint gradient was then compared with that from the finite difference calculated using Eq. (3). This equation was selected in order to save CPU time by minimizing the number of forward model function calculations. For this test we used $\varepsilon = 0.01$."

5996.15: The sentence is unclear and needs rephrasing. How exactly are you saving CPU time here?

The sentence was revised as follows: "The adjoint gradient was then compared with that from the finite difference calculated using Eq. (3). This equation was selected in order to save CPU time by minimizing the number of forward model function calculations. For this test we used $\varepsilon = 0.01$."

In Eq. (3) evaluates perturbations at point $(x+\varepsilon)$. Eq. (4) evaluates perturbations at points $(x+\varepsilon)$ and $(x-\varepsilon)$. Thus, Eq. (4) requires a two times more simulations with forward model.

5997.17: This section needs more explanation. What simulations did you carry out here, exactly? What were your initial conditions for the adjoint model runs?

We added: "$CO_2$ initial conditions and fluxes were the same as those used for the CELGA forward simulations in Section 4"

We revised the section entirely.

6013-14: Keep the same order of cases from left to right when printing R, M and S in the plots (i.e. red-cs1, blue-cs2, green-cs3, not green, blue, red).

Done

Figures 4 – 7: It might be interesting to see panels showing the differences between the different results when using the different versions of the model, as it can be difficult to discern these differences by eye. Also, in Figure 5, are the left-hand and right-hand panels the same results, but aggregated onto different grids? I can see the logic of this, but it feels a little unnecessary to me to have both grids displayed. I'd consider showing only the results on the native model grid, as Figure 6 shows the combined results on the 2.5 degree grid anyway.

It is difficult to show differences between the different results when using the different versions of the model, because they have a different spatial extension. We tried to make the figures easier to compare and combined them. The section revised.

Technical corrections: Overall, the manuscript requires a thorough proofreading in order to make sure that there are no further technical corrections necessary. I have included all of the mistakes that I found.

Done

5984.7: tangent -> tangent linear

Revised

5984.11: As results -> As a result

Revised

5984.17: shown -> shows that

Revised

5984.20: demonstrates the high accuracy -> demonstrates high accuracy

Revised

5985.18: a density of observational network -> the densityof the observational network

Revised

5985.21: CO2 observation are not existing -> CO2 observations do not exist

Revised

5986.13: If tracer is a chemically inert -> if a tracer is chemically inert

Revised

5986.15: is running -> is run

Revised

5986.28: speeds -> speeds up

Revised

5987.10: To utilize of the strongest sides of both methods -> In order to exploit the advantages of both methods

Revised

5988.10: This may change in the font of the final manuscript, but the capital "I" and lower-case "l" appear identical in this equation. Maybe consider changing notation?

Revised. "L" and "l" are replaced with "S" and "s" correspondently.

5989.12: The model's employs -> The model employs

Revised

5989.16: we follows -> we follow

Revised

5989.22: ration -> ratio

Revised

5989.25: intercomparisons -> comparisons

Revised

5990.2: FLEXPART similar to other LPDMs consider … -> FLEXPART, like other LPDMs, considers ...

Revised

5990.4: sink and sources -> sinks and sources

Revised

5990.5: running -> tracking? following?

Revised

5990.6: no comma necessary here

Revised

5990.11: Gaussian grid T106 -> Gaussian T106 grid

Revised

5990.12: and in 6h time steps -> and 6-hourly time steps.

Revised

5991.2: 3-dimensional -> 3D

Revised

5991.6: driving -> driven

Revised

5991.8: “The” current version

Revised

5991.10: Remove extra ‘of’

Revised

5991.13: parameter estimation method used in different reanalysis dataset the use. . .

-> parameter estimation methods used in different reanalysis datasets, the use

Revised

5994.21: a construction of continuous adjoint -> construction of a continuous adjoint

Revised

5995.13: remoted -> remote (or distanced?)

Revised

5995.20: inpute -> input

Revised

5997.2: did not seriously changed -> did not significantly change

Revised

5997.8: the M in the denominator should be M’ (i.e. tangent linear)

Revised

6000.12: Performed in the paper analyses showed, that GELCA -> Analyses in this paper showed that GELCA. . .

Revised

6000.14: Decreasing of the Eulerian model resolution are not able to significantly distort. . .
-> Decreasing the Eulerian model resolution does not significantly distort. . .

Revised

6001.3: variation -> variational

Revised

6014: As Fig 2 -> As Fig 1

Revised

6015: Siberian observations towers -> Siberian observation towers

Revised

REFERENCES:

Hooghiemstra, P. B., M. C. Krol, T. T. van Leeuwen, G. R. van der Werf, P. C. Novelli, M. N. Deeter, I. Aben, and T. Röckmann (2012), Interannual variability of carbon monoxide emission estimates over South America from 2006 to 2010, J. Geophys. Res., 117, D15308, doi:10.1029/2012JD017758.

# Adjoint of the Global Eulerian–Lagrangian Coupled Atmospheric transport model (A-GELCA v1.0): development and validation

**D.A. Belikov[1,2,3], S. Maksyutov[1], A. Yaremchuk[4], A. Ganshin[3,5], T. Kaminski[6,*], S. ~~Blessing~~[6]Blessing[7], M. Sasakawa[1], Angel J. Gomez-Pelaez[8] and A. Starchenko[3]**

[1]{National Institute for Environmental Studies, Tsukuba, Japan}

[2]{National Institute of Polar Research, Tokyo, Japan}

[3]{Tomsk State University, Tomsk, Russia}

[4]{N. Andreev Acoustic Institute, Moscow, Russia}

[5]{Central Aerological Observatory, Dolgoprudny, Russia}

[6]{The Inversion Lab, Hamburg, Germany}

[7]{FastOpt GmbH, Hamburg, Germany}

~~[*]{now~~[8]{Izaña Atmospheric Research Center (IARC), Meteorological State Agency of Spain (AEMET), Izaña, 38311, Spain}

[*]{Previously at: ~~The Inversion Lab~~FastOpt GmbH, Hamburg, Germany~~} }~~

Correspondence to: D.A. Belikov (dmitry.belikov@nies.go.jp)

## Abstract

We ~~present~~presented the development of the Adjoint of the Global Eulerian–Lagrangian Coupled Atmospheric (A-GELCA) model that consists of the National Institute for Environmental Studies (NIES) model as an Eulerian three-dimensional transport model (TM), and FLEXPART (FLEXible PARTicle dispersion model) as the Lagrangian ~~plume diffusion model~~Particle Dispersion Model (LPDM).

The forward tangent linear and adjoint components of the Eulerian model were constructed directly from the original NIES TM code using an automatic differentiation tool known as TAF (Transformation of Algorithms in Fortran; http://www.FastOpt.com), with additional manual pre- and post-processing aimed at improving transparency and clarity of the code and optimizing the performance of the computing, including MPI (Message Passing Interface). ~~As results, the adjoint of Eulerian model is discrete. Construction of the adjoint of the~~The Lagrangian component did not require any code modification, as LPDMs are ~~able to~~self-adjoint and track a significant number of particles ~~back~~backwad in time ~~and thereby~~in order to calculate the sensitivity of the observations to the neighboring ~~emissions~~emission areas. The constructed Eulerian ~~and~~adjoint was coupled with the Lagrangian ~~adjoint components were coupled~~ component at ~~the~~a time boundary in the global domain.~~The results are verified~~ The simulations presented in this work were performed using ~~a series of test experiments.~~the A-GELCA model in forward and adjoint modes. The forward simulation ~~shown~~shows that the coupled model ~~is effective in~~improves reproducing of the seasonal cycle and short-term variability of $CO_2$ ~~even in the case of multiple limiting factors, such as high uncertainty of fluxes and the low resolution~~ . The adjoint of the Eulerian model~~. The adjoint model demonstrates the high accuracy~~ was shown, through several numerical tests, to be very accurate compared to direct forward sensitivity calculations~~ and fast performance~~. The developed adjoint of the coupled model combines the flux conservation and stability of an Eulerian discrete adjoint formulation with the flexibility, accuracy, and high resolution of a Lagrangian backward trajectory formulation. A-GELCA will be incorporated into a variational inversion system designed to optimize surface fluxes of greenhouse gases.



**Keywords:** atmospheric transport and inverse modeling, adjoint model, carbon cycle

## 1. Introduction

Forecasts of $CO_2$ levels in the atmosphere and predictions of future climate depend on our scientific understanding of the natural carbon cycle (IPCC, 2007; Peters et al., 2007). To estimate the spatial and temporal distribution of carbon sources and sinks, inverse methods are used to infer carbon fluxes from geographically sparse observations of the atmospheric $CO_2$ mixing ratio (Tans et al., 1989). The first comprehensive efforts in atmospheric $CO_2$ inversions date back to the late 1980s and early 1990s (Enting and Mansbridge, 1989; Tans et al., 1989). With the increase in spatial coverage of $CO_2$ observations and the development of ~~3D~~three-dimentional (3-D) tracer transport models, a variety of numerical experiments and projects have been performed by members of the so-called "TransCom" community of inverse modelers (e.g., Law et al., 1996, 2008; Denning et al., 1999; Gurney et al., 2002, 2004; Baker et al., 2006; Patra et al., 2011). A number of studies have proposed improvements to the inverse methods of atmospheric transport ~~(~~, i.e. the efficient computation of the transport matrix by the model adjoint proposed by Kaminski et al~~,~~. (1999b~~;~~), use of monthly mean GLOBALVIEW-$CO_2$ ground-based data (current version is for 2014) by Rödenbeck et al~~,~~. (2003~~;~~), development an ensemble data assimilation method by Peters et al~~,~~. (2005~~;~~), flux inversion at high temporal (daily) and spatial (model grid) resolution using for the first time of continuous $CO_2$ measurements over Europe by Peylin et al~~,~~. (2005~~;~~), use satellite data to constrain the inversion of $CO_2$ by Chevallier et al~~,~~. (2005~~; Meirink et al., 2008;~~), develop of a new observational screening technique by Maki et al~~,~~. (2010). Despite progress in atmospheric $CO_2$ inversions, a recent intercomparison (Peylin et al., 2013) demonstrated the need for further refinement.

In recent decades, ~~a~~the density of the observational network established to monitor greenhouse gases in the atmosphere has been increased, and more measurements taken onboard ships and aircraft are becoming available (~~Bovensmann~~Karion et al., ~~1999).~~2013; Tohjima et al., 2015). However, on a global scale $CO_2$ ~~observation are~~observations do not ~~existing~~exist for many remote regions not covered by networks. This lack of data is one of the main limitations of atmospheric inversions, which can be filled by monitoring from space (Rayner and O'Brien, 2001). The satellite observation data from current (GOSAT, Kuze et al., 2009; Yokota et al., 2009; OCO-2, Crisp et al., 2004) and future missions (CarbonSat/CarbonSat Constellation; Bovensmann et al., 2010; Buchwitz et al., 2013) offer enormous potential for $CO_2$ inverse modeling. Optimal application of large observed datasets requires expanding the inverse analysis of $CO_2$ to finer resolution, higher precision and faster

performance.

To link surface fluxes of $CO_2$ to observed atmospheric concentrations, an accurate model of atmospheric transport and an inverse modeling technique are needed. Generally, ~~there are the Eulerian and the Lagrangian method of modelling~~ the atmospheric constituents transport may be described in two different ways: the Lagrangian and the Eulerian approaches. The Eulerian method treats the atmospheric tracers as a continuum on a control volume basis, so it is more effective ~~in~~ reproducing of long-term patterns, i.e. the seasonal cycle or the interhemispheric gradient. The Lagrangian Particle Dispersion Models (LPDMs) consider atmospheric tracers as a discrete phase and tracks each individual particle, therefore LPDMs are better for resolving synoptic and hourly variations.

To relate fluxes and concentrations of ~~a~~ long-lived species like $CO_2$, a transport model must cover a long simulation period (e.g., Bruhwiler et al., 2005). Therefore, computing time is a critical issue and minimization of the computational cost is essential. ~~If tracer is a~~For chemically inert tracers, the transport can be represented by a model's Jacobian matrix, because the simulated concentration at observational sites is a linear function of the flux sets. ~~To~~ Theoretically, to compute such ~~a~~ matrix ~~a~~the transport model is ~~running~~run multiple times with set of prescribed surface fluxes. However, this would require an extremely large number of forward model evaluations. The adjoint of the transport model is an efficient way to ~~evaluate derivatives~~accelerate calculation of concentration gradient of the simulated tracer at observational locations ~~towards to the sources and sinks of tracer~~ (Kaminski et al., 1999).

Marchuk (1974) first applied the adjoint approach in atmospheric science. After that, this method became widely used in meteorology. In the 1990s the use of this approach was expanded to the field of tracer transport modeling (Elbern et al., 1997; Kaminski et al., 1999).

Adjoint models have numerous applications, including the data assimilation of concentrations, inverse modeling of chemical source strengths, sensitivity analysis, and parameter sensitivity estimation (Enting, 2002; Haines et al., 2014). Recent studies have used this method to constrain estimates of the emissions of ~~various tracers~~$CO_2$ using retrieved column integrals from the ~~GOME and MOPITT~~GOSAT satellite ~~instruments (Müller and Stavrakou, 2005; Kopacz~~(Basu et al., ~~2009~~2013; Deng et al., 2014; Liu et al., 2015).

Using the adjoint model speeds up the process of inverse modeling. However, high CPU and memory demands prevent us from using Eulerian chemical transport models (CTMs) with high-resolution grids in inversions. It would be beneficial to increase the model resolution close to observation points, where ~~small uncertainties in~~ the ~~transport~~strong

observation constraint can ~~seriously~~significantly improve the optimization of the resulting emission fluxes.

LPDM running in the backward mode can explicitly estimate a source–receptor sensitivity matrix by solving the adjoint equations of atmospheric transport (Stohl et al., 2009), which is mathematically presented by a Jacobian expressing the sensitivity of concentration at the observational locations. Marchuk (1995), and Hourdin and Talagrand (2006) ~~discussed the~~provided derivations proving equivalence of the adjoint of forward transport models to backward transport models.

~~To utilize of~~In order to exploit the ~~strongest sides~~advantages of both methods, Lagrangian and Eulerian chemical transport models can be coupled to develop ~~the~~an adjoint, ~~which~~that is suitable for the simultaneous ~~estimation of~~simulation of contributions from global and regional emissions. Coupling can be performed in several ways; e.g., a regional-scale LPDM can be coupled to a global Eulerian model at ~~the~~a regional domain boundary (Rödenbeck et al., 2009; Rigby et al., 2011), or a global-scale LPDM can be coupled to an Eulerian model at the time boundary (Koyama et al., 2011; Thompson and Stohl, 2014).

~~One~~The goal of this study is to present the development and evaluation of an Adjoint of the Global Eulerian–Lagrangian Coupled Atmospheric model (A-GELCA), which consists of an Eulerian National Institute for Environmental Studies global Transport Model (NIES-TM; Maksyutov et al., 2008; Belikov et al., 2011, 2013a, 2013b) and a Lagrangian particle dispersion model (FLEXPART; Stohl et al., 2005). This approach utilizes the accurate transport of the LPDM to calculate the signal near to the receptors, and ~~rapid~~efficient calculation of background responses using the adjoint of the Eulerian global transport model. In contrast to previous works (Rödenbeck et al., 2009; Rigby et al., 2011; Thompson and Stohl, 2014), in which the regional models were coupled at the spatial boundary of the domain, we implemented a coupling at ~~the~~a time boundary in the global model domain (as described in Sect. 2.1). A-GELCA can be integrated into a variational inverse modeling system designed to optimize surface fluxes.

The remainder of this paper is organized as follows. An overview of the coupled model is provided in Sect. 2~~, and in~~. In Sect. 3 we describe the variational inversion ~~process~~scheme. In Sect. 4 we address several problems regarding the coupled model that have not been covered previously (Ganshin et al., 2012). In Sect. 5 we describe the formulation and evaluation of the adjoint model. The computational efficiency of the adjoint model is analyzed in Sect. 6, and ~~finally~~ the conclusions are presented in Sect. 7.

1

## 2. Model and method

### ~~3.~~2.1. Global coupled Eulerian-Lagrangian model

In ~~the~~this paper we use a global Eulerian-Lagrangian coupled model, the principles of which are described by Ganshin et al. (2012). ~~In this section we provide the formula~~The coupled model consists of FLEXPART (version 8.0; run in backward mode) as the Lagrangian particle dispersion model, and NIES TM (version NIES-08.1i) as the Eulerian off-line global transport model. For concentration $C(x_r, t_r)$ (mole fraction) at receptor point $x_r$ and time $t_r$ we provide the equation in its discrete form, as implemented in the model for the case of surface fluxes:

~~$$C(x_r,t_r) = \frac{Tm_{air}}{hNL\rho m_{CO_2}} \sum_{ij}^{IJ} \sum_{l=0}^{L} F_{ij}^{l} \sum_{n=1}^{N} f_{ij}^{\ln} + \frac{1}{N} \sum_{ijk}^{IJK} C_{ijk}^{B} \sum_{n=1}^{N} f_{ijk}^{n}, \quad (1)$$~~

$$C(x_r, t_r) = \frac{Tm_{air}}{hNS\rho m_{CO_2}} \sum_{ij}^{IJ} \sum_{s=0}^{S} F_{ij}^{s} \sum_{n=1}^{N} f_{ij}^{sn} + \frac{1}{N} \sum_{ijk}^{IJK} C_{ijk}^{B} \sum_{n=1}^{N} f_{ijk}^{n}, \quad (1)$$

where *i, j,* and *k* are the indices that characterize the ~~position~~location of ~~the particle in~~ ~~the~~each grid cell; ~~l~~s is the time index; ~~p is the particle index; $F_{ij}^{l}$~~ $F_{ij}^{l}$ are the surface fluxes in $kg \cdot m^{-2} \cdot s^{-1}$; ~~$C_{ijk}^{B}$~~ $C_{ijk}^{B}$ are the background concentrations ~~in~~calculated by the Eulerian model~~; $f_{ijk}^{n}$~~ at the coupling time; $f_{ijk}^{n}$ equals unity if the particle is within cell *i, j, k*, otherwise it equals zero; *T* is the duration of the backward trajectory; ~~L~~S is the number of steps in time; *N* is the total number of particles; *h* is the height up to which the effect of the surface fluxes is considered significant; $\rho$ is the average air density below height *h*; and $m_{\text{air}}$ and $m_{CO2}$ are the molar masses of air and carbon dioxide, respectively. ~~The FLEXPART model starts at the observation point and calculates seven days' worth of backward trajectories for 1000 air particles, which are dispersed under the influence of turbulent diffusion. The background grid values of the concentrations, which are interpolated to the final points of the back trajectories, are transferred to the observation point and are the second term in the right-hand side of Eq. (1).~~ The first term in this formula describes the contribution of the nearby sources of the ~~component~~ considered component; these sources are located along the trajectories inside layer h (500 m). The value of the first term is proportional to the flux in each cell along the trajectory, and to the time during which the air particle is inside this cell (Ganshin et al., ~~2013). We implemented a coupling at the time boundary in the global domain~~2012). The background grid values of the concentrations (calculated by the Eulerian model), which are

interpolated to the final points of the backward trajectories, are transferred to the observation point and are the second term in the right-hand side of Eq. (1). The FLEXPART model starts simulation at the observation point and calculates seven-day backward trajectories for 1000 air particles, which are dispersed under the influence of turbulent diffusion. The number of particles has been chosen to optimize the computational cost without compromising the quality of modeling by Ganshin et al., (2013). The scheme of concentration calculation for the given location includes coupling of two model approaches. NIES TM calculates global concentrations for the selected time period (usually 1 year to exclude spin-up effect), but stops 7 days before the time of the observations. To obtain the concentrations for the observation time we transport the background concentrations from NIES TM gridbox to the location of observation point along the trajectory ensemble calculated by FLEXPART model and add contribution from surface sources. Therefore we have implemented the coupling at a time boundary in the global domain of the NIES transport model, while nested regional modeling systems such as one by Rodenbeck et al (2009) have to couple at both region boundary and time boundary.

~~The coupled model consists of FLEXPART (version 8.0; run in backward mode) as the Lagrangian particle dispersion model, and NIES TM (version NIES-08.1i) as the Eulerian off-line global transport model to calculate the background $CO_2$ values.~~

### ~~3.1. NIES transport model~~

Since the first publication of the GELCA model in 2012, the NIES transport model has undergone significant updates. We provide a brief outline of the major features of the current model. NIES TM is a global three-dimensional CTM that simulates the global distribution of atmospheric tracers between the Earth's surface and a pressure level of 5 hPa. The ~~model's~~model employs the standard horizontal latitude–longitude grid with reduced number of meshes towards the poles and a spatial resolution of 2.5° × 2.5° near the equator(Belikov et al., 2011). The vertical coordinate is a flexible hybrid sigma–isentropic (σ–θ) with 32 levels (Belikov et al., 2013b). To parameterize turbulent diffusivity we ~~follows~~follow the method proposed by Hack et al. (1993), with a separate evaluation of transport processes in the free troposphere and the planetary boundary layer (PBL). The PBL heights are provided by the European Centre for Medium-Range Weather Forecasts (ECMWF) ERA-Interim reanalysis. The modified Kuo-type parameterization scheme is used for cumulus convection (Belikov et al., 2013a).

Inverse modeling assumes that the model reasonably well reproduces the relationship

between atmospheric mixing ~~ration~~ratio and surface fluxes, assuming that the biases between the simulated and observed concentrations are mostly due to the emission inventories errors. To ensure that this is the case, the NIES TM model has been evaluated extensively~~, and it consistently performs well in intercomparisons~~. Comparisons against $SF_6$ and $CO_2$ (Belikov et al., 2011, 2013b), $CH_4$ (Patra et al., 2011; Belikov et al., 2013b), and $^{222}Rn$ (Belikov et al., 2013a) measurements show the model ability to reproduce seasonal variations, interhemispheric gradient and vertical profiles of tracers.

#### ~~3.2.~~2.2. FLEXPART

FLEXPART ~~similar to~~, like other LPDMs ~~consider~~, considers atmospheric tracers as ~~a discrete phase~~ clouds of individual particles and tracks ~~pathways~~the pathway of each ~~individual~~ particle. The advantage of this approach is the direct estimation of the sensitivity of the measurements to the neighboring ~~sink~~sinks and sources by ~~running~~tracking the particles ~~back~~backward in time. Usually it is ~~enough~~sufficient to simulate for a limited number of days (2-10) to determine~~,~~ where particles intercept the surface layer before they spread vertically and horizontally.

#### ~~3.3.~~2.3. Meteorological data

To run both models we use reanalysis ~~which combines~~dataset combining the Japanese 25-yr Reanalysis (JRA-25) and the Japanese Meteorological Agency Climate Data Assimilation System (JCDAS) dataset (Onogi et al., 2007). The JRA-25/JCDAS dataset is distributed on a Gaussian T106 grid ~~T106~~ with horizontal resolution 1.25° × 1.25°, 40 sigma-pressure levels and in 6-~~h~~hour time steps. The use of JRA-25/JCDAS data for Eulerian and Lagrangian models provides ~~a~~ consistency in the calculated fields; however, some features of FLEXPART and NIES TM require different methods for processing the meteorological data.

##### ~~3.3.1.~~2.3.1. *Meteorological data processing for NIES TM*

Isolation of the transport equations is an effective way to save a significant amount of CPU time during tracer transport simulation. At the preprocessing stage, the NIES TM core produced a static archive of advective, diffusive, and convective mass fluxes with time step similar to the one of the original JRA-25/JCDAS data (6 hour). After that the archive is used by an "offline" model specially designed only for passive transport of tracer. Intermediate fluxes are derived by interpolation.

Besides the mass fluxes, the static archives contain fields of temperature, pressure,

humidity, vertical grid parameters (variation of the sigma-isentropic vertical coordinate over time), and others. The pre-calculated and stored data field can be used directly for any of the inert tracers. It is also possible to simulate chemically active tracers if the chemical reaction can be written in the ~~simplified~~linear decay form; e.g., for $^{222}Rn$, $CH_4$. Approximately 20 3-~~dimensional~~D and 1-dimensional arrays are written to a hard disk for every record. This comprises around 10 GB of data per modelled month for the model's standard resolution of 2.5° × 2.5°.

### ~~3.3.2.~~2.3.2. *Meteorological data processing for FLEXPART*

Originally, FLEXPART was ~~driving~~driven by ECMWF reanalysis dataset distributed on a grid with regular latitude–longitude horizontal structure and sigma–pressure vertical coordinate. ~~Current~~The current version of the model was adapted to use JRA-25/JCDAS data, by horizontal bilinear interpolation of the required parameters from a Gaussian grid to a regular 1.25 × 1.25 grid. The vertical structure and temporal resolution of ~~of~~ JRA-25/JCDAS data were used without modification.

Given the large differences in structure, resolution and parameter estimation ~~method~~methods used in different reanalysis dataset, the use of the same meteorology for both Eulerian and Lagrangian models ~~is a~~provides significant benefit.

## ~~4.~~3. Inverse modeling for the flux optimization problem

Although the variational inversion method ~~theory~~ for minimizing the discrepancy between modeled and observed mixing ratios has been well described and published (i.e. Chevallier et al., 2005), we summarize it here.

The aim of the ~~inverse~~inversion problem is to find the value of a state vector $\mathbf{x}$ with $n$ elements that minimizes ~~a~~the cost function $J(x)$ ~~using a least-squares method:~~):

~~$$J(\mathbf{x}) = \frac{1}{2}(\mathbf{x}-\mathbf{x}_b)^T \mathbf{B}^{-1}(\mathbf{x}-\mathbf{x}_b) + \frac{1}{2}(\mathbf{Hx}-\mathbf{y})^T \mathbf{R}^{-1}(\mathbf{Hx}-\mathbf{y}),$$~~

$$J(\mathbf{x}) = \frac{1}{2}(\mathbf{x}-\mathbf{x}_b)^T \mathbf{B}^{-1}(\mathbf{x}-\mathbf{x}_b) + \frac{1}{2}(\mathbf{Hx}-\mathbf{y})^T \mathbf{R}^{-1}(\mathbf{Hx}-\mathbf{y}), \quad (2)$$

where $\mathbf{y}$ is a vector of observations with $m$ elements, and the matrix $\mathbf{H}$ represents the forward model simulation mapping the state vector $\mathbf{x}$ to the observation space. Here, ~~**R**~~ **R** is the covariance matrix (size $m \times m$) for observational error, which includes instrument and representation errors. The matrix ~~**R**~~ **R** also includes errors of the forward model $\mathbf{H}$. ~~**B**~~ **B** is the covariance matrix (size $n \times n$) of error for prior information of the state vector $\mathbf{x}_b$. ~~Use~~The use of the cost function in the form of Eq. (2) assumes that all errors ~~must~~ have Gaussian statistics and ~~be~~are unbiased (Rodgers, 2000).

~~For linear **H,**~~ The minimization of the cost function (Eq. 2) has an analytic solution ~~involving~~that involves a matrix inversion. If the Jacobian $\mathbf{H}$ is available this analytic solution can implemented, unless the matrix sizes are too large for the available computing resources. Alternatively, Eq. 2 can be solved through an iterative minimization algorithm. In this case, the existence of the gradient of $J(\mathbf{x})$ with respect to $\mathbf{x}$ allows using of powerful gradient algorithms for ~~minimisation~~minimization. This gradient is efficiently provided by the adjoint (Giering and Kaminski, 1998; Kaminski et al., 1999; Chevallier et al., 2005~~; Kopacz et al., 2009).~~).

## ~~5.~~4. Assessment of the coupled model

The effect of different horizontal resolutions on Eulerian models is discussed in detail by Patra et al. (2008). In general, higher resolution helps to resolve a more detailed distribution of the tracer. However, the use of a ~~more detailed~~higher resolution grid leads to additional computational cost, which is not always justified by the resulting model output. ~~This is~~Higher resolution does not produce better results largely due to the limited availability of high-resolution meteorology and tracer emission datasets.

The paper by Ganshin et al. (2012) ~~in various test showed that~~describing the

~~coupled~~development of the GELCA model ~~surpasses the Eulerian~~provides a model ~~in 4-month simulations~~testing report. The advantage of GELCA in reproducing the high-concentration spikes and short-term variations caused mainly by anthropogenic emissions is more vivid ~~with use of~~when using high resolution (1 km × 1 km) surface fluxes compared to standard ~~low~~ resolution (1° × 1°) fluxes. However those tests considered only short 4-month simulations for a limited number of locations.

We ~~repeated~~expanded the comparison undertaken by Ganshin et al. (2012) ~~for~~to a two-year period using an updated set of prescribed fluxes, which combines four components similar to the analysis performed by Takagi et al~~.,~~ (2011) and Maksyutov et al~~., (2012~~. (2013): (a) anthropogenic fluxes from the Open source Data Inventory of Anthropogenic $CO_2$ (ODIAC; Oda and Maksyutov, 2011) and the Carbon Dioxide Information Analysis Center's (CDIAC; Andres et al., 2009, 2011) datasets; (b) biosphere fluxes simulated by the Vegetation Integrative SImulator for Trace gases (VISIT) terrestrial biosphere model (Ito, 2010; Saito et al., 2011, 2013); (c) oceanic fluxes predicted by a data assimilation system based on the Offline ocean Tracer Transport Model (OTTM; Valsala and Maksyutov, 2010); and (d) biomass burning emissions from the Global Fire Emissions Database (GFED) version 3.1 (van der Werf et al., 2010). Biosphere fluxes have daily time step, while the others are monthly. The initial global CO2 distribution was obtained from GLOBALVIEW-CO2 (2014).

We considered several cases with different model resolutions. For NIES TM we tested grids at 10.0°, 2.5°, and 1.25° resolutions, with FLEXPART running at 1.0° (Table 1). The resolution of the input fluxes was matched to that of FLEXPART. ~~Modeled~~Model results were compared with observations from the World Data Centre for Greenhouse Gases (WDCGG 2015) and the Siberian observations obtained by the Center for Global Environmental Research (CGER) of the National Institute for Environmental Studies (NIES) and the Russian Academy of Science (RAS), from ~~seven~~six tower sites (JR-STATION) as described ~~in Table 2 (~~by Sasakawa et al~~.,~~. (2010). The selected site locations are shown in Fig. 1.

Although the total number of observational stations contributing to the WDCGG is about several hundreds, the set of sites conducting continuous (high temporal resolution is needed for the coupled model) observations is much smaller. We selected 19 sites (Table 2). Most of them are concentrated in the temperate latitudes of the northern hemisphere, where the variations in $CO_2$ concentration are most noticeable.

Siberia is assumed to be a substantial source and sink of $CO_2$ ~~emissions~~, with high uncertainties in the fluxes describing them (McGuire et al., 2009; Hayes et al., 2011; Saeki et

al., 2013). As a result, CTMs tend to reproduce the ~~interseasonal~~interannual variability of $CO_2$ quite poorly. We selected six tower JR-STATION sites to check the model performance in the Siberian region (Table 3).

The analyzed sites are divided into three groups. The first group includes remote and marine sites (ALT, AMS, BRW, CPT, IZO, JBN, MLO, MNM, ZEP) with very weak influence of local sources, so the seasonal variation of CO2 is controlled by global, large-scale variations. For these sites contribution by using the Lagrangian component is negligible (see Fig. 2-4 panel b to analyze the difference between the coupled and the Eulerian models).

The second group includes sites with domination of long term variability of $CO_2$ and relatively smooth and weak short term variations. Typically, these sites are located on the border of two regions with very different fluxes (AMY, CMN, MHD, PAL, PRS, YON).

The sites selected to the third group are strongly influenced by local emissions and global transport at the same time. Therefore the $CO_2$ concentration variation is controlled by the strength and direction of wind, the depth of the boundary layer and other factors. Such sites are mainly in the northern mid-latitudes (HUN, PUY, SSL, WSA) including all Siberian towers (DEM, IGR, KRS, NOY, VGN, YAK). For these locations contributions of the Eulerian and Lagrangian components are comparable. Therefore, the coupled model introduces the most significant improvement when simulating $CO_2$ for these sites.

Figures ~~2 and 3 compare~~5 compares the coupled and Eulerian model results with ~~tower~~ observations from the Igrim and Vaganovo~~. Recent~~ towers. The recent modifications ~~(~~indicated in Sect. 2.2~~) mean that~~ have significantly improve the performance of NIES TM ~~is significantly improved~~ compared with the results reported by Ganshin et al. (2012). However, ~~in this case~~compared to the updated NIES TM the coupled model ~~reproduces the observations~~is better ~~than the Eulerian model used on its own, providing a~~reproducing short term peaks of concentration. This explains the observed reduction of the mean bias and STD (up to 1.5 ppm), and the better simulation of the seasonal variation (in phase and ~~its~~ amplitude~~. The standard deviation of the coupled~~). The improvements in the CO2 simulations due to the addition of the Lagrangian component to the Eulerian model ~~misfit to the observations is around 0.5 ppm smaller. Moreover, the version of the coupled model with a very coarse grid of NIES TM (10.0°) outperforms the~~ are higher~~-~~ than those obtained by increasing the resolution ~~versions~~ of the Eulerian NIES transport model (~~Table 3~~Fig. 2-4). Given the huge difference in computation costs between NIES TM for low- and high-resolution grids (i.e. a difference by a factor of ~15 between grids with resolution 10.0° and 2.5°), the

advantage of the GELCA model is clear. Performance is important, as the setup considered here is almost identical to ~~the case~~that used in the inverse modeling of $CO_2$.

However, improvements in $CO_2$ simulation due to the implementation of the GELCA model were obtained not for all the considered sites. This ~~case~~ shows that further modification of the setup (i.e. more detail meteorological data, switch to higher resolution) is necessary. Nevertheless, the coupled model is an effective ~~even in the case of multiple limiting factors, such as high uncertainty of fluxes, a small number~~way to improve simulation of ~~observations, and~~$CO_2$ without increasing the ~~low~~ resolution of the Eulerian model. We recognize that ~~the~~is quite problematic to use ~~of the concentrations simulated from~~ the highly uncertain surface fluxes to ~~judge~~simulate the tracer concentrations and use these concentrations for estimating the quality of different model configurations ~~is quite problematic~~. Nevertheless, we cannot improve our analysis, because we do not have concentration measurements for tracers ~~with more accurate~~whose surface fluxes are more accurately known, like SF6.

## ~~6.~~5. Construction and validation of the adjoint model

### ~~6.1.~~5.1. Construction

In this section, we present the development of the adjoint of the coupled model. ~~Construction~~The incorporation of the ~~adjoint to the~~ Lagrangian ~~part~~component does not require any modification to the code, as LPDMs are ~~able to track a significant number of particles backwards in time and thereby calculate the sensitivity of observations to the neighboring emissions areas.~~

self-adjoint. The development of the adjoint ~~to~~of the Eulerian part is more complicated. We decided to develop a discrete adjoint of NIES TM in order to make it consistent with the forward model. An alternative approach is ~~a~~the construction of a continuous adjoint derived from the leading equations of the forward model (Giles and Pierce, 2000). The main advantage of the discrete adjoint model is that the resulting gradients of the numerical cost function are exact, even for nonlinear or iterative algorithms, ~~making them~~and this makes easier to validate~~, as validation of~~ the adjoint model, which is an essential and complicated task.

The ~~tangent linear and~~ adjoint ~~models~~model for NIES TM ~~were~~was created manually to achieve maximum computational efficiency, while the adjoint of NIES TM to FLEXPART coupler was created using the Transformation of Algorithms in Fortran (TAF) software

(http://www.FastOpt.com). ~~Use~~However, the use of this tool required some manual treatment of the code. ~~We~~TAF successfully produces the tangent linear and adjoint code of individual procedures, but it gets confused when the model has complex structures (such as loops and conditional operators). Therefore we often manually ~~redesign~~redesigned and ~~optimize~~optimized the automatically generated adjoint code to optimize the efficiency ~~and~~, improve readability and clarity of the adjoint model and optimize the performance of computing using MPI, as the TAF code used here (version 1.5) do not fully support MPI routines.

The advantages of our coupled adjoint model are as follows.

1. Simple ~~construction~~incorporation of the Lagrangian part ~~of the adjoint, as~~, since no modification of the LPDM is ~~not~~ required. Potentially, NIES TM can be coupled to any Lagrangian model.
2. ~~Minimizing~~Minimization of the simulation time can be obtained, as once calculated the output from the Lagrangian model is applicable for different long-lived tracers.
3. Reduction of aggregation errors can be achieved, as the sensitivity for small regions and even individual model cells near to observation sites is estimated using the LPDM part, while the sensitivity for large regions ~~remoted~~remote from the monitoring sites is derived using the Eulerian part (Kaminski et al., 2001).
4. ~~Minimizing~~Minimization of the computational cost can be obtained, as high-resolution simulation are performed over a limited number of regions nearby to the observational sites using the LPDM part, while for the rest of the globe the coarse-resolution results are calculated by the Eulerian part.
5. High consistency of ~~calculated~~the tracer ~~field~~fields calculated by the Lagrangian and the Eulerian models due to the fact that both models use ~~of~~ the same ~~impute~~input meteorology.

The main drawback of the method is that the deriving of discrete adjoint of Eulerian model is a significant technical challenge.

### ~~6.2.~~5.2. Validation of the coupled adjoint

An essential stage of the adjoint model construction is its validation. A lack of accuracy in the adjoint model ~~is~~will likely ~~to~~ degrade the performance of the ~~minimisation of~~ cost function minimization (Eq. 2~~.~~). Several different tests were carried out to evaluate the

accuracy and precision of the constructed adjoint model ~~calculation~~. Considering ~~a~~the simple formulation of the ~~adjoint for the~~ Lagrangian part, we focused on testing the NIES TM adjoint.

### ~~6.2.1.~~5.2.1. *Validation of the NIES TM adjoint*

The discrete adjoint obtained through automatic differentiation can be easily validated by comparing the adjoint sensitivities with forward model gradients calculated using the finite difference approximation (Henze at al., 2007).

~~Forward~~The forward model sensitivity, ~~λ~~$\lambda_F$, is calculated using the one- or two-sided finite difference equation,

$$\lambda = \frac{M'(x+\varepsilon) - M'(x)}{\varepsilon} \quad \lambda_F = \frac{M'(x+\varepsilon) - M'(x)}{\varepsilon} \tag{3}$$

$$\lambda = \frac{M'(x+\varepsilon) - M'(x-\varepsilon)}{2\varepsilon} \tag{4}$$

$$\lambda_F = \frac{M'(x+\varepsilon) - M'(x-\varepsilon)}{2\varepsilon} \tag{4}$$

where $M$` denotes the tangent linear model. A range of $\varepsilon$ = 0.1–0.01 was proved in most cases to give an optimal balance between truncation and roundoff error (Henze at al., 2007).

In the first test, ~~forward~~adjoint simulations were carried out ~~with~~using an initial $CO_2$ distribution ~~and~~, zero surface flux for 2 days ~~using~~ (1-2 January 2010) and a horizontal grid with resolution 2.5° × 2.5°. ~~Adjoint simulations were then performed with $CO_2$ distribution perturbed by 1 ppm per grid cell.~~ The adjoint gradient was then compared with that from the finite difference calculated using Eq. (3~~)~~). This equation was selected in order to save CPU time by minimizing the number of forward model function ~~calculation for the case~~calculations. For this test we used $\varepsilon$ = 0.01.

To quantify the difference between the two calculations of the sensitivity λ, we define the local relative error

$$E(\text{lon}, \text{lat}) = \frac{|\lambda_A - \lambda_F|}{\max \lambda_A}, \tag{5}$$

$$E(lon, lat) = \frac{|\lambda_A - \lambda_F|}{max\ \lambda_A}, \tag{5}$$

where the subscripts A and F refer to adjoint and finite difference respectively, whereas *lon*~~,~~ and *lat*, ~~–~~refer to longitude and latitude ~~correspondently.~~, respectively. Figure ~~3c~~6c shows *E(lon, lat)* with a logarithmic color scale. The sensitivities obtained ~~by~~for the adjoint have maximum relative error of order $10^{-16}$, indicating that transport in the NIES TM adjoint is

correct over short timescales. The overall comparisons did not seriously ~~changed~~change if we select ~~a~~ different grid cells or use ~~various~~other values of $\varepsilon$.

The definition of the adjoint of the tangent linear forward model M* requires that for an inner product ~~$\langle , \rangle$~~ $\langle , \rangle$ and two random vectors **u** and **v**, the following expression should ~~be valid~~hold:

~~$\forall \mathbf{u}, \forall \mathbf{v} \ \langle M'\mathbf{u}, \mathbf{v} \rangle = \langle \mathbf{u}, M^*\mathbf{v} \rangle.$~~ $\forall \mathbf{u}, \forall \mathbf{v} \ \langle M'\mathbf{u}, \mathbf{v} \rangle = \langle \mathbf{u}, M^*\mathbf{v} \rangle.$ (6)

For practical use the identity in Eq. (6) is ~~reworded~~rewritten as follows (Wilson et al., 2014):

~~$\frac{\|M'(\mathbf{u})\|^2}{\left(\mathbf{u}, M^*\left(M\left(\mathbf{u}\right)\right)\right)} = 1.$~~ (7)

$\frac{\|M'(\mathbf{u})\|^2}{\left(\mathbf{u}, M^*\left(M'(\mathbf{u})\right)\right)} = 1.$ (7)

We use Eq. (7) to test the adjoint model initialized using several different random ~~setups.~~random vectors **u** and **v**. For all cases, Eq. (7) compares well ~~with~~within machine epsilon with mismatch between -3e$^{-14}$ to 6e$^{-14}$.

### ~~6.2.2.~~5.2.2. *Real case simulation*

The next series of calculations was made for real measurements. ~~As in the first part of the article, we~~ We used data from the Siberian observation network ~~(Table 2)~~(Table 3) for the period 1–4 January 2010. ~~The NIES adjoint was simulated with a horizontal resolution of 2.5° × 2.5°,~~$CO_2$ initial conditions and ~~the Lagrangian response was simulated with a horizontal~~ fluxes were the same as those used for the CELGA forward simulations in Section 4. We run A-GELCA using grids of 10.0° and 2.5° for Eulerian part and of 1.0° for Lagrangian component (similar to Cs-1 and Cs-2 in Table 1) and considered several cases.

The sensitivities of $CO_2$ concentrations were calculated using the Eulerian component only in Figs. 7,8 a) (resolution of 2.5º), b) (resolution of ~~1.0° × 1.0°.~~

~~Figure 4 shows the sensitivity calculated with the Eulerian component, while Fig. 5 shows the same but~~ 10.0º), using the Lagrangian component~~. Although the contours of the two figures coincide, it is clear~~ only in Figs. 7,8 c)(resolution of 1.0º), and d) (resolution of 1.0º, but aggregated on a grid with resolution of 2.5º), and using the coupled adjoint model in

Fig. 7,8 e) (Eulerian component at a resolution of 2.5º and the Lagrangian component aggregated on the grid with a resolution of 2.5º), and f) (as for e) , but the resolution of the Eulerian adjoint model was 10.0º). Figure 7 corresponds to the 2-nd day of simulation, while Figure 8 is for 4-th day.

Above, we have already stated that the Eulerian part of the coupled model is more effective in reproducing of long-term patterns, while the Lagrangian part is better for resolving synoptic and hourly variations. This follows from the fact that the A-GELCA components have different footprints. The Eulerian adjoint has a wider footprint, with the greatest ~~value~~values in an area where the effect of all stations is summed. ~~In this case, most of the stations can be outside this zone, as the~~ The Euler model monitors global and large-scale changes~~. This figure illustrates~~, although some stations can be outside this zone (i.e. YAK, at Fig. 7a,g or NOY, at Fig. 8a,b). These figures illustrate why the Eulerian model, even with a sufficiently detailed grid, ~~is unable~~fails to reproduce $CO_2$ variations (Sect. 4). The footprint width decreases when the NIES TM resolution is increased, but the value of the sensitivity increases ~~with resolution~~.

The FLEXPART model sensitivity shows more irregular distributions, and higher values closer to the observational sites, thereby reflecting the model's ability to monitor small-scale changes~~.~~ (Fig. 7-8 panels c,d).

During coupling, the sensitivity is aligned due to the crosslinking of components (Fig. ~~6~~7-8 panels e,f). Thus, the intensity has ~~a~~ maximum near the stations and smoothly decreases ~~with increasing~~when distance increases. The Eulerian and Lagrangian models employ different approaches and grid resolutions for the modeling of atmospheric tracers, and can thus resolve processes with different time and spatial scales, and underlying physics.

~~Figure 7 shows the sensitivity calculated for the same setup as for Fig. 6, but using NIES TM with a 10.0° resolution.~~ By changing the Eulerian model resolution, it is possible to change size of the footprint. This system can utilize responses calculated at higher resolutions, such as 0.5° or 0.1°, but these setups require more accurate driving data and regular observations available for smaller time steps.

## ~~7.~~6. Computational efficiency

We tested several different methods to reduce the computational ~~burden~~cost of the adjoint model. First, the Eulerian part of the adjoint model was driven by static archives of

meteorological parameters, as described in Sect. 2.4.1. Second, the forward NIES model was altered so that at each model timestep it saved any variables that ~~would~~were also ~~be~~ needed by the adjoint model. ~~These~~Therefore, these variables ~~therefore~~ did not have to be recalculated for ~~use~~being used in the adjoint model. ~~(~~This was possible because we used a discrete version of the adjoint, which was fully compatible with the forward model~~).~~ Third, the Lagrangian part of the adjoint model made use of pre-calculated response functions, as described in Sect. 2.4.2.

To run the adjoint model we used a Linux workstation with 8 Intel(R) Xeon(R) E5-4650 2.~~70GHz~~70 GHz processors and 64 GB of RAM. The CPU time of the adjoint model (backward only) ~~is~~was almost equal to CPU time required to run the forward model. It ~~takes~~took about 1.3 min for a ~~weeklong~~week-long iteration (forward and backward). The memory demand ~~is~~was about 1 GB. Henze et al. (2007) reports that the ratio between simulation time in backward and forward modes for adjoint models derived for other CTMs, as follows: GEOS-Chem: 1.5, STEM: 1.5, CHIMERE: 3–4, IM-AGES: 4, Polair: 4.5–7, and CIT: 11.75. Thus, the adjoint of the developed coupled model GELCA is quite efficient. To achieve this level of efficiency, a substantial amount of manual programming effort is required, despite the automatic code generated by TAF. The main disadvantage of TAF is that many redundant recomputations are often generated by the compiler. A crucial optimization of the adjoint code is required to eliminate these extra recomputations.

## ~~8.~~7. Summary

In this ~~papers~~paper we have presented the construction and evaluation of an adjoint of the global Eulerian–Lagrangian coupled model GELCA that will be integrated into a variational inverse system designed to ~~optimizing~~optimize surface fluxes. The coupled model combines the NIES three-dimensional transport model as its Eulerian part and the FLEXPART plume diffusion model as its Lagrangian component. The Eulerian and Lagrangian components are coupled at a time boundary in the global domain. The model was originally developed to study the carbon dioxide and methane atmospheric ~~distribution~~distributions.

The Lagrangian component did not require any code modification, as FLEXPART is ~~tracking~~a self-adjoint and tracks a significant number of particles ~~back~~backward in time~~, and thereby calculates~~ in order to calculate the sensitivity of observations to the neighboring emissions areas. ~~Thus, construction of the adjoint to the Lagrangian part does not require any modification to the code.~~

For Eulerian part, the discrete adjoint was constructed directly from the original NIES TM code, ~~in contrast to a construction of~~instead of contrasting a continuous adjoint derived from the forward model basic equations. The tangent linear and adjoint models of the ~~Eulerian model~~NIES TM to FLEXPART coupler were derived using the automatic differentiation software TAF (http://www.FastOpt.com), which significantly accelerated the development. However, considerable manual processing of forward and adjoint model codes was necessary to improve the transparency and clarity of the model and to optimize the computational performance of ~~computing~~, including MPI~~. The~~, as the TAF code used here (version 1.5) ~~did~~does not fully support MPI routines.

~~The Eulerian and Lagrangian adjoints were coupled at the time boundary in the global domain.~~ The main benefit of the developed discrete adjoint is accurate calculation of the numerical cost function gradients, even if the algorithms are nonlinear. The overall advantages of the developed model also include relatively simple ~~construction~~incorporation of the ~~adjoint to the~~ Lagrangian part and fast computation using the Lagrangian component, scalability of sensitivity calculation depending on distance to monitoring sites, thereby reducing aggregation errors, and computational efficiency even for high-resolution simulations.

The ~~accuracy of the~~ transport scheme accuracy of the forward coupled model was investigated using ~~simulation of~~the distribution of the atmospheric $CO_2$. The GELCA components and the model itself had previously been validated ~~in~~using various tests and by

comparison with ~~both~~ measurements and with other transport models for $CO_2$ and other tracers. ~~Performed~~The analyses in the present paper ~~analyses showed,~~have shown that ~~GELCA~~CELGA is effective in capturing the seasonal variability of atmospheric tracer at observation sites. Decreasing of the Eulerian model resolution ~~are~~does not ~~able to~~ significantly distort the transport model performance~~;~~, however, running the coupled model using NIES TM with low resolution grid can maximize simulation speed and use of data storage.

The Eulerian ~~and Lagrangian components of the~~ adjoint ~~model were~~was validated using various tests in which the adjoint gradients were compared to gradients calculated with numerical finite difference. We evaluated each ~~individual~~ routine of the discrete adjoint of the Eulerian model and the adjoint gradients of the cost function. The ~~obtained~~ precision obtained of the results ~~in~~of the considered numerical experiments demonstrates proper construction of the adjoint.

The CPU time ~~of~~needed by the adjoint model is comparable with ~~that~~those of other models, as we used several methods to reduce the computational ~~load~~cost. The forward NIES model was altered so that at each model ~~timestep~~time step it saved ~~any~~all variables that ~~would~~were also ~~be~~being needed by the adjoint model. These variables therefore did not have to be recalculated for use in the adjoint model. In addition, the adjoint simulation was isolated from the recalculation of NIES TM meteorological parameters and Lagrangian response functions. All supplementary parameters ~~are~~were pre-calculated before running the adjoint and ~~are~~were stored in static archives.

The developed ~~adjoint~~A-GELCA model will be incorporated into ~~variation~~a variational inversion system aiming studying greenhouse gases (mainly $CH_4$ and $CO_2$), by assimilating tracer measurements from *in situ*, aircraft and remote sensing observations. However, before performing real inverse modeling simulations it is necessary to select a proper minimization program and find the optimal values for the error covariance matrices **R** and **B** ~~with the optimal values~~.

## Code availability

All code in the current version of the NIES forward model is available on request. Any potential user interested in these modules should contact D. Belikov~~,~~ (dmitry.belikov@nies.go.jp) or S. Maksyutov (shamil@nies.go.jp), and any feedback on the modules is welcome. Note that ~~one~~that potential users may need help using the forward and adjoint model effectively, but open support for the model is not available due to lack of resources. The code of the adjoint part of the current NIES model is unavailable for distribution, as it was generated using the commercial tool TAF (http://www.FastOpt.com). However, we can provide the sources which were used as input for TAF.

The FLEXPART code was taken from the official web site http://flexpart.eu/. The procedures necessary to run FLEXPART with the JCDAS reanalysis are also available upon request.

## Acknowledgments

The authors thank A. Stohl for providing the FLEXPART model. We also thank T. Machida for Siberian observation data (downloaded from http://db.cger.nies.go.jp/). The JRA-25/JCDAS meteorological datasets used in the simulations were provided by the Japan Meteorological Agency. The WDCGG observation data used in the comparisons were provided by The World Data Centre for Greenhouse Gases. The computational resources were provided by NIES. This study was ~~performed~~supported by order of the Ministry for Education and Science of the Russian Federation No. 5.628.2014/K~~ and was supported~~ by ~~The~~the Tomsk State University Academic D.I. Mendeleev Fund Program in 2014–2015 and by GRENE Arctic project.

## References


Andres, R. J., Boden, T. A., and Marland, G.: Annual fossil-fuel CO2 emissions: Mass of emissions gridded by one degree latitude by one degree longitude. Carbon Dioxide Information Analysis Center, Oak Ridge National Laboratory, U.S. Department of Energy, Oak Ridge, Tenn., U.S.A., doi 10.3334/CDIAC/ffe.ndp058.2009, 2009.

Andres, R. J., Gregg, J. S., Losey, L., Marland, G., Boden, T.: Monthly, global emissions of carbon dioxide from fossil fuel consumption, Tellus 63B, 309–327, 2011.

Baker, D. F., Law, R. M., Gurney, K. R., Rayner, P., Peylin, P., Denning, A. S., Bousquet, P., Bruhwiler, L., Chen, Y.-H., Ciais, P., Fung, I. Y., Heimann, M., John, J., Maki, T., Maksyutov, S., Masarie, K., Prather, M., Pak, B., Taguchi, S., and Zhu, Z.: TransCom 3 inversion intercomparison: impact of transport model errors on the interannual variability of regional $CO_2$ fluxes, 1988–2003, Global Biogeochem. Cy., 20, GB1002, doi:10.1029/2004GB002439, 2006.

Basu, S., Guerlet, S., Butz, A., Houweling, S., Hasekamp, O., Aben, I., Krummel, P., Steele, P., Langenfelds, R., Torn, M., Biraud, S., Stephens, B., Andrews, A., and Worthy, D.: Global CO2 fluxes estimated from GOSAT retrievals of total column CO2, Atmos. Chem. Phys., 13, 8695-8717, doi:10.5194/acp-13-8695-2013, 2013.

Belikov, D., Maksyutov, S., Miyasaka, T., Saeki, T., Zhuravlev, R., and Kiryushov, B.: Mass-conserving tracer transport modelling on a reduced latitude-longitude grid with NIES-TM, Geosci. Model Dev., 4, 207–222, 2011.

Belikov, D. A., Maksyutov, S., Krol, M., Fraser, A., Rigby, M., Bian, H., Agusti-Panareda, A., Bergmann, D., Bousquet, P., Cameron-Smith, P., Chipperfield, M. P., Fortems-Cheiney, A., Gloor, E., Haynes, K., Hess, P., Houweling, S., Kawa, S. R., Law, R. M., Loh, Z., Meng, L., Palmer, P. I., Patra, P. K., Prinn, R. G., Saito, R., and Wilson, C.: Off-line algorithm for calculation of vertical tracer transport in the troposphere due to deep convection, Atmos. Chem. Phys., 13, 1093–1114, doi:10.5194/acp-13-1093-2013, 2013a.

Belikov, D., Maksyutov, S., Sherlock, V., Aoki, S., Deutscher, N. M., Dohe, S., Griffith, D., Kyro, E., Morino, I., Nakazawa, T., Notholt, J., Rettinger, M., Schneider, M., Sussmann, R., Toon, G. C., Wennberg, P. O., and Wunch, D.: Simulations of column-average $CO_2$ and $CH_4$ using the NIES TM with a hybrid sigma–isentropic (σ–θ) vertical coordinate, Atmos. Chem. Phys., 13, 1713–1732, doi:10.5194/acp-13-1713-2013, 2013b.

Bovensmann, H., Burrows, J. P., Buchwitz, M., Frerick, J., Noël, S., Rozanov, V. V., Chance, K. V., and Goede, A. P. H.: SCIAMACHY: Mission objectives and measurement modes, J. Atmos. Sci., 56, 127–150, 1999.

Bovensmann, H., Buchwitz, M., Burrows, J. P., Reuter, M., Krings, T., Gerilowski, K., Schneising, O., Heymann, J., Tretner, A., and Erzinger, J.: A remote sensing technique for global monitoring of power plant $CO_2$ emissions from space and related applications, Atmos. Meas. Tech., 3, 781–811, doi:10.5194/amt-3-781-2010, 2010.

Bruhwiler, L. M. P., Michalak, A. M., Peters, W., Baker, D. F., and Tans, P. P.: An improved

Kalman Smoother for atmospheric inversions, Atmos. Chem. Phys., 5, 2691–2702, doi:10.5194/acp-5- 2691-2005, 2005.

Buchwitz, M., Reuter, M., Bovensmann, H., Pillai, D., Heymann, J., Schneising, O., Rozanov, V., Krings, T., Burrows, J. P., Boesch, H., Gerbig, C., Meijer, Y., and Löscher, A.: Carbon Monitoring Satellite (CarbonSat): assessment of atmospheric $CO_2$ and $CH_4$ retrieval errors by error parameterization, Atmos. Meas. Tech., 6, 3477–3500, doi:10.5194/amt-6-3477-2013, 2013.

Chevallier, F., Fisher, M., Peylin, P., Serrar, S., Bousquet, P., Bréon, F.-M., Chédin, A., and Ciais, P.: Inferring $CO_2$ sources and sinks from satellite observations: method and application to TOVS data, J. Geophys. Res., 110, D24309, doi:10.1029/2005JD006390, 2005.

Crisp, D., Atlas, R. M., Bréon, F.-M., Brown, L. R., Burrows, J. P., Ciais, P., Connor, B. J., Doney, S. C., Fung, I. Y., Jacob, D. J., Miller, C. E., O'Brien, D., Pawson, S., Randerson, J. T., Rayner, P., Salawitch, R. S., Sander, S. P., Sen, B., Stephens, G. L., Tans, P. P., Toon, G. C., Wennberg, P. O., Wofsy, S. C., Yung, Y. L., Kuang, Z., Chudasama, B., Sprague, G., Weiss, P., Pollock, R., Kenyon, D., and Schroll, S.: The Orbiting Carbon Observatory (OCO) mission, Adv. Space Res., 34, 700–709, 2004.

Deng, F., Jones, D. B. A., Henze, D. K., Bousserez, N., Bowman, K. W., Fisher, J. B., Nassar, R., O'Dell, C., Wunch, D., Wennberg, P. O., Kort, E. A., Wofsy, S. C., Blumenstock, T., Deutscher, N. M., Griffith, D. W. T., Hase, F., Heikkinen, P., Sherlock, V., Strong, K., Sussmann, R., and Warneke, T.: Inferring regional sources and sinks of atmospheric CO2 from GOSAT XCO2 data, Atmos. Chem. Phys., 14, 3703-3727, doi:10.5194/acp-14-3703-2014, 2014.

Elbern, H., Schmidt, H., and Ebel, A.: Variational data assimilation for tropospheric chemistry modeling, J. Geophys. Res., 102, 15,967–15,985, 1997.

Enting, I. G., and Mansbridge, J. V., Seasonal sources and sinks of atmospheric $CO_2$: Direct inversion of filtered data, Tellus B, 41B, 111–126, doi: 10.1111/j.1600-0889.1989.tb00129.x, 1989.

Enting, I. T.: Inverse problems in atmospheric constituent transport, Cambridge University Press, Cambridge, UK, 2002.

Ganshin, A., Oda, T., Saito, M., Maksyutov, S., Valsala, V., Andres, R. J., Fisher, R. E., Lowry, D., Lukyanov, A., Matsueda, H., Nisbet, E. G., Rigby, M., Sawa, Y., Toumi, R., Tsuboi, K., Varlagin, A., and Zhuravlev, R.: A global coupled Eulerian-Lagrangian model and 1 × 1 km $CO_2$ surface flux dataset for high-resolution atmospheric $CO_2$ transport simulations, Geosci. Model Dev., 5, 231–243, doi:10.5194/gmd-5-231-2012, 2012.

Giles, M. B., and Pierce, N. A.: An Introduction to the Adjoint Approach to Design, Flow Turbul. Combust., 65, 393–415, 2000.

Giering, R., and T. Kaminski, Recipes for adjoint code construction, Trans. Math. Software, 24(4), 437–474, doi:10.1145/293686.293695, 1998.

GLOBALVIEW-CO2 Cooperative Atmospheric Data Integration Project - Carbon Dioxide. CD-ROM, NOAA ESRL, Boulder, Colorado [Also available on Internet via anonymous FTP to

ftp.cmdl.noaa.gov, Path: ccg/co2/GLOBALVIEW], 2014.

Gurney, K. R., Law, R. M., Denning, A. S., Rayner, P. J., Baker, D., Bousquet, P., Bruhwilerk, L., Chen, Y.-H., Ciais, P., Fan, S., Fung, I., Gloor, M., Heimann, M., Higuchi, K., John, J., Maki, T., Maksyutov, S., Masarie, K., Peylin, P., Prather, M., Pak, B. C., Randerson, J. R., Sarmiento, J., Taguchi, S., Takahashi, T. and Yuen, C.-W.: Towards robust regional estimates of $CO_2$ sources and sinks using atmospheric transport models, Nature, 415, 626–630, 2002.

Gurney, K. R., Law, R. M., Denning, A. S., Rayner, P. J., Pak, B. C., Baker, D., Bousquet, P., Bruhwiler, L., Chen, Y.-H., Ciais, P., Fung, I. Y., Heimann, M., John, J., Maki, T., Maksyutov, S., Peylin, P., Prather, M., and Taguchi, S.: Transcom 3 inversion intercomparison: model mean results for the estimation of seasonal carbon sources and sinks, Global Biogeochem. Cy., 18, GB1010, doi:10.1029/2003GB002111, 2004.

Hack, J. J., Boville, B. A., Briegleb, B. P., Kiehl, J. T., Rasch, P. J., and Williamson, D. L.: Description of the NCAR community climate model (CCM2), NCAR/TN-382, 108, 1993.

Haines, P. E., Esler, J. G., and Carver, G. D.: Technical note: Adjoint formulation of the TOMCAT atmospheric scheme in the Eulerian backtracking framework (RETRO-TOM), Atmos. Chem. Phys., 14, 5477–5493, 2014.

Hayes, D. J., McGuire, A. D., Kicklighter, D. W., Gurney, K. R., Burnside, T. J., and Melillo, J. M.: Is the northern high-latitude land-based $CO_2$ sink weakening?, Global Biogeochem. Cycles, 25, GB3018, doi:10.1029/2010GB003813, 2011.

Henze, D. K., Hakami, A., and Seinfeld, J. H.: Development of the adjoint of GEOS-Chem, Atmos. Chem. Phys., 7, 2413–2433, doi:10.5194/acp-7-2413-2007, 2007.

Hourdin, F., and Talagrand, O.: Eulerian backtracking of atmospheric tracers. I: Adjoint derivation and parametrization of subgid-scale transport, Q. J. Roy. Meteor. Soc., 132, 585–603, 2006.

IPCC 2007: Climate change 2007: the physical science basis, in: Contribution of Working Group I to the Fourth Assessment Report of the Intergovernmental Panel on Climate Change (eds. Solomon, S., Qin, D., Manning, M., Chen, Z., Marquis, M., et al.), Cambridge University Press, Cambridge, pp. 135–145.

Ito, A.: Changing ecophysiological processes and carbon budget in East Asian ecosystems under near-future changes in climate: Implications for long-term monitoring from a process-based model, J. Plant Res., 123, 577–588, 2010.

Kaminski, T., Heimann, M., and Giering, R.: A coarse grid three-dimensional global inverse model of the atmospheric transport: 1. Adjoint model and Jacobian matrix, J. Geophys. Res., 104(D15), 18,535–18,553, doi:10.1029/1999JD900147, 1999a.

Kaminski, T., Heimann, M., and Giering, R.: A coarse grid three-dimensional global inverse model of the atmospheric transport: 2. Inversion of the transport of CO2 in the 1980s, J. Geophys. Res., 104(D15), 18,555-18,581, doi:10.1029/1999JD900146, 1999b.

Kaminski, T., Rayner, P., Heimann, M., and Enting, I.: On aggregation errors in atmospheric transport inversions, J. Geophys. Res., 106(D5):4703, 2001.

Karion, A., Sweeney, C., Wolter, S., Newberger, T., Chen, H., Andrews, A., Kofler, J., Neff, D., and Tans, P.: Long-term greenhouse gas measurements from aircraft, Atmos. Meas. Tech., 6, 511-526, doi:10.5194/amt-6-511-2013, 2013.

Koyama, Y., Maksyutov, S., Mukai, H., Thoning, K., and Tans, P.: Simulation of variability in atmospheric carbon dioxide using a global coupled Eulerian–Lagrangian transport model, Geosci. Model Dev., 4, 317–324, doi:10.5194/gmd-4-317-2011, 2011.

Kuze, A., Suto H., Nakajima M., and Hamazaki T.: Thermal and near infrared sensor for carbon observation Fourier-transform spectrometer on the Greenhouse Gases Observing Satellite for greenhouse gases monitoring, Appl. Opt., 48, 6716–6733, doi:10.1364/AO.48.006716, 2009.

~~Kopacz, M., Jacob, D. J., Henze, D. K., Heald, C. L., Streets, D. G., and Zhang, Q.: Comparison of adjoint and analytical Bayesian inversion methods for constraining Asian sources of carbon monoxide using satellite (MOPITT) measurements of CO columns, J. Geophys. Res., 114, D04305, doi:10.1029/2007JD009264, 2009.~~

~~Koyama, Y., Maksyutov, S., Mukai, H., Thoning, K., and Tans, P.: Simulation of variability in atmospheric carbon dioxide using a global coupled Eulerian–Lagrangian transport model, Geosci. Model Dev., 4, 317–324, doi:10.5194/gmd-4-317-2011, 2011.~~

Law, R. M., Rayner, P. J., Denning, A. S., Erickson, D., Fung, I. Y., Heimann, M., Piper, S. C., Ramonet, M., Taguchi, S., Taylor, J. A., Trudinger, C. M., and Watterson, I. G.: Variations in modelled atmospheric transport of carbon dioxide and the consequences for $CO_2$ inversions, Global Biogeochem. Cy., 10, 783–796, 1996.

Law, R. M., Peters, W., Rödenbeck, C., Aulagnier, C., Baker, I., Bergmann, D. J., Bousquet, P., Brandt, J., Bruhwiler, L., Cameron-Smith, P. J., Christensen, J. H., Delage, F., Denning, A. S., Fan, S., Geels, C., Houweling, S., Imasu, R., Karstens, U., Kawa, S. R., Kleist, J., Krol, M. C., Lin, S.-J., Lokupitiya, R., Maki, T., Maksyutov, S., Niwa, Y., Onishi, R., Parazoo, N., Patra, P. K., Pieterse, G., Rivier, L., Satoh, M., Serrar, S., Taguchi, S., Takigawa, M., Vautard, R., Vermeulen, A. T., and Zhu, Z.: TransCom model simulations of hourly atmospheric $CO_2$: Experimental overview and diurnal cycle results for 2002, Global Biogeochem. Cy., 22, GB3009, doi:10.1029/2007GB003050, 2008.

Liu, J., Bowman, K. W., and Henze D. K.: Source-receptor relationships of column-average CO2 and implications for the impact of observations on flux inversions. J. Geophys. Res. Atmos., 120, 5214–5236. doi: 10.1002/2014JD022914, 2015.

Maki, T., Ikegami, M., Fujita, T., Hirahara, T., Yamada, K., Mori, K., Takeuchi, A., Tsutsumi, Y., Suda, K., and Conway, T. J., New technique to analyse global distributions of $CO_2$ concentrations and fluxes from non-processed observational data, Tellus B, 62, 797–809, doi:10.1111/j.1600-0889.2010.00488.x, 2010.

Maksyutov, S., Patra, P. K., Onishi, R., Saeki, T., and Nakazawa, T.: NIES/FRCGC Global Atmospheric Tracer Transport Model: Description, validation, and surface sources and sinks inversion, J. Earth Simulator, 9, 3–18, 2008.

Maksyutov, S., Takagi, H., Valsala, V. K., Saito, M., Oda, T., Saeki, T., Belikov, D. A., Saito, R., Ito, A., Yoshida, Y., Morino, I., Uchino, O., Andres, R. J., and Yokota, T.: Regional $CO_2$ flux estimates for 2009–2010 based on GOSAT and groundbased $CO_2$ observations, Atmos. Chem. Phys., 13, 9351–9373. http://dx.doi.org/10.5194/acp-13-9351-2013, 2013.

Marchuk, G.: Numerical solution of the problems of the dynamics of the atmosphere and the ocean (In Russian), Gidrometeoizdat, Leningrad, 303 pp., 1974.

Marchuk, G. I.: Adjoint equations and analysis of complex systems, Series: Mathematics and its applications, v. 295, Kluwer Academic Publishers, Dordrecht and Boston, 484 pp., 1995.

McGuire, A. D., Anderson, L. G., Christensen, T. R., Dallimore, S., Guo, L. D., Hayes, D. J., Heimann, M., Lorenson, T. D., Macdonald, R. W., and Roulet, N.: Sensitivity of the carbon cycle in the Arctic to climate change, Ecol. Monogr., 79(4), 523–555, doi:10.1890/08-2025.1, 2009.

~~Meirink, J. F., Bergamaschi, P., Frankenberg, C., d'Amelio, M. T. S., Dlugokencky, E. J., Gatti, L. V., Houweling, S., Miller, J. B., Roeckmann, T., Villani, M. G., and Krol, M. C.: Four-dimensional variational data assimilation for inverse modeling of atmospheric methane emissions: Analysis of SCIAMACHY observations, J. Geophys. Res., 113, doi:10.1029/2007JD009740, 2008.~~

~~Müller, J.-F., and Stavrakou, T.: Inversion of CO and NOx emissions using the adjoint of the IMAGES model, Atmos. Chem. Phys., 5, 1157–1186, doi:10.5194/acp-5-1157-2005, 2005.~~

Oda, T., and Maksyutov, S.: A very high-resolution (1 km × 1 km) global fossil fuel $CO_2$ emission inventory derived using a point source database and satellite observations of nighttime lights, Atmos. Chem. Phys., 11, 543–556, doi:10.5194/acp-11-543-2011, 2011.

Onogi, K., Tsutsui, J., Koide, H., Sakamoto, M., Kobayashi, S., Hatsushika, H., Matsumoto, T., Yamazaki, N., Kamahori, H., Takahashi, K., Kadokura, S., Wada, K., Kato, K., Oyama, R., Ose, T., Mannoji, N., and Taira, R.: The JRA-25 Reanalysis, J. Meteor. Soc. Japan, 85, 369–432, 2007.

Patra, P. K., Law, R. M., Peters, W., Rodenbeck, C., Takigawa, M., Aulagnier, C., Baker, I., Bergmann, D. J., Bousquet, P., Brandt, J., Bruhwiler, L., Cameron-Smith, P. J., Christensen, J. H., Delage, F., Denning, A. S., Fan, S., Geels, C., Houweling, S., Imasu, R., Karstens, U., Kawa, S. R., Kleist, J., Krol, M. C., Lin, S.-J., Lokupitiya, R., Maki, T., Maksyutov, S., Niwa, Y., Onishi, R., Parazoo, N., Pieterse, G., River, L., Satoh, M., Serrar, S., Taguchi, S., Vautard, R., Vermeulen, A. T., and Zhu, Z.: TransCom model simulations of hourly atmospheric $CO_2$: Analysis of synoptic-scale variations for the period 2002–2003, Global Biogeochem. Cy., 22, GB4013, doi:10.1029/2007GB003081, 2008.

Patra, P. K., Houweling, S., Krol, M., Bousquet, P., Belikov, D., Bergmann, D., Bian, H., Cameron-Smith, P., Chipperfield, M. P., Corbin, K., Fortems-Cheiney, A., Fraser, A., Gloor, E., Hess, P., Ito, A., Kawa, S. R., Law, R. M., Loh, Z., Maksyutov, S., Meng, L., Palmer, P. I., Prinn, R. G., Rigby, M., Saito, R., and Wilson, C.: TransCom model simulations of $CH_4$ and related species: linking transport, surface flux and chemical loss with $CH_4$ variability in the troposphere and lower stratosphere, Atmos. Chem. Phys., 11, 12813–12837,

doi:10.5194/acp-11-12813-2011, 2011.

Peters, W., Miller, J. B., Whitaker, J., Denning, A. S., Hirsch, A., Krol, M. C., Zupanski, D., Bruhwiler, L., and Tans, P. P.: An ensemble data assimilation system to estimate $CO_2$ surface fluxes from atmospheric trace gas observations, J. Geophys. Res., 110, D24304, doi:10.1029/2005JD006157, 2005.

Peters, W., ~~Jacobson, A. R., Sweeney, C., Andrews, A. E., Conway, T. J., Masarie, K.,~~ Miller, J~~. B., Bruhwiler, L., M. P., Pétron, G.~~, Whitaker, J., Denning, S., Hirsch, A~~. I., Worthy, D. E. J., van der Werf, G. R., Randerson, J. T., Wennberg, P. O~~., Krol, M~~. C., ~~., Zupanski, D., Bruhwiler, L., and Tans, P~~. P~~.: An ensemble data assimilation system to estimate $CO_2$ surface fluxes from atmospheric trace gas observations, J. Geophys. Res., ~~perspective on North American carbon dioxide exchange: CarbonTracker, Proc. Nat. Academy Sci., 104, 18,925–18,930, doi:10.1073/pnas.0708986104, 2007.~~110, D24304, doi:10.1029/2005JD006157., 2005. Peylin, P., Rayner, P. J., Bousquet, P., Carouge, C., Hourdin, F., Heinrich, P., Ciais, P., and AEROCARB contributors: Daily $CO_2$ flux estimates over Europe from continuous atmospheric measurements: 1, inverse methodology, Atmos. Chem. Phys., 5, 3173–3186, doi:10.5194/acp-5-3173-2005, 2005.

Peylin, P., Law, R. M., Gurney, K. R., Chevallier, F., Jacobson, A. R., Maki, T., Niwa, Y., Patra, P. K., Peters, W., Rayner, P. J., Rödenbeck, C., and Zhang, X.: Global atmospheric carbon budget: results from an ensemble of atmospheric $CO_2$ inversions, Biogeosciences Discuss., 10, 5301–5360, doi:10.5194/bgd-10-5301-2013, 2013.

Rayner P. J., and O'Brien, D. M.: The utility of remotely sensed $CO_2$ concentration data in surface source inversions, Geophys. Res. Lett., 28, 175–178, 2001.

Rigby, M., Manning, A. J., and Prinn, R. G.: Inversion of long-lived trace gas emissions using combined Eulerian and Lagrangian chemical transport models, Atmos. Chem. Phys., 11, 9887–9898, doi:10.5194/acp-11-9887-2011, 2011.

Rodgers, C. D.: Inverse methods for atmospheric sounding, vol. 2 of Series on Atmospheric, Oceanic and Planetary Physics, World Scientific, Singapore, 2000.

Rödenbeck, C., Houweling, S., Gloor, M., and Heimann, M.: ~~Time-dependent~~$CO_2$ flux history 1982–2001 inferred from atmospheric ~~$CO_2$ inversions based on interannually varying tracer~~data using a global inversion of atmospheric transport, ~~Tellus B, 55, 488–497~~Atmos. Chem. Phys., 3, 1919–1964, doi:10.5194/acp-3-1919-2003, 2003.

Rödenbeck, C., Gerbig, C., Trusilova, K., and Heimann, M.: A two-step scheme for high-resolution regional atmospheric trace gas inversions based on independent models, Atmos. Chem. Phys., 9, 5331–5342, doi:10.5194/acp-9-5331-2009, 2009.

Saito, M., Ito, A., and Maksyutov, S.: Evaluation of biases in JRA-25/JCDAS precipitation and their impact on the global terrestrial carbon balance, J. Climate, 24, 4109–4125, 2011.

Saito, M., Ito, A., and Maksyutov, S.: Optimization of a prognostic biosphere model in atmospheric $CO_2$ variability and terrestrial biomass, Geosci. Model Dev. Discuss., 6, 4243–4280, doi:10.5194/gmdd-6-4243-2013, 2013.

Saeki, T., Maksyutov, S., Sasakawa, M., Machida, T., Arshinov, M., Tans, P., Conway, T. J., Saito, M., Valsala, V., Oda, T., Andres, R. J., and Belikov, D.: Carbon flux estimation for Siberia by inverse modeling constrained by aircraft and tower $CO_2$ measurements, J. Geophys. Res. Atmos., 118, doi:10.1002/jgrd.50127, 2013.

Sasakawa, M., K. Shimoyama, T. Machida, N. Tsuda, H. Suto, M. Arshinov, D. Davydov, A. Fofonov, O. Krasnov, T. Saeki, Y. Koyama, and S. Maksyutov, Continuous measurements of methane from a tower network over Siberia, Tellus 62B, 403–416, 2010.

Stohl, A., Forster, C., Frank, A., Seibert, P., and Wotawa, G.: Technical note: The Lagrangian particle dispersion model FLEXPART version 6.2, Atmos. Chem. Phys., 5, 2461–2474, doi:10.5194/acp-5-2461-2005, 2005.

Stohl, A., Seibert, P., Arduini, J., Eckhardt, S., Fraser, P., Greally, B. R., Lunder, C., Maione, M., Mhle, J., O'Doherty, S., Prinn, R. G., Reimann, S., Saito, T., Schmidbauer, N., Simmonds, P. G., Vollmer, M. K., Weiss, R. F., and Yokouchi, Y.: An analytical inversion method for determining regional and global emissions of greenhouse gases: Sensitivity studies and application to halocarbons, Atmos. Chem. Phys., 9, 1597–1620, doi:10.5194/acp-9-1597-2009, 2009.

Takagi, H., Saeki, T., Oda, T., Saito, M., Valsala, V., Belikov, D., Saito, R., Yoshida, Y., Morino, I., Uchino, O., Andres, R. J., Yokota, T., and Maksyutov, S.: On the benefit of GOSAT observations to the estimation of regional $CO_2$ fluxes, SOLA, 7, 161–164, 2011.

Tans, P. P., Conway, T. J., and Nakazawa, T.: Latitudinal distribution of the sources and sinks of atmospheric carbon dioxide derived from surface observations and an atmospheric transport model, J. Geophys. Res., 94, 5151–5172, 1989.

Tarantola, A.: Inverse Problem Theory and Methods for Model Parameter Estimation, Society for Industrial and Applied Mathematics, Philadelphia, USA, 2005.

Thompson, R. L., and Stohl, A.: FLEXINVERT: an atmospheric Bayesian inversion framework for determining surface fluxes of trace species using an optimized grid, Geosci. Model Dev., 7, 2223–2242, doi:10.5194/gmd-7-2223-2014, 2014.

~~Valsala, V., and Maksyutov, S.: Interannual variability of the air–sea $CO_2$ flux in the north Indian Ocean, Ocean Dynam., 63, 165–178, doi:10.1007/s10236-012-0588-7, 2013.~~

Tohjima, Y., Terao, Y., Mukai, H., Machida, T., Nojiri, Y., & Maksyutov, S.: ENSO-related variability in latitudinal distribution of annual mean atmospheric potential oxygen (APO) in the equatorial Western Pacific. Tellus B, 67. doi:http://dx.doi.org/10.3402/tellusb.v67.25869, 2015.

Valsala V. and Maksyutov S.: Simulation and assimilation of global ocean $pCO_2$ and air-sea $CO_2$ fluxes using ship observations of surface ocean $pCO_2$ in a simplified biogeochemical offline model, Tellus-B, 62B, 821–840, doi:10.1111/j.1600-0889.2010.00495.x, 2010.

van der Werf, G. R., Randerson, J. T., Giglio, L., Collatz, G. J., Mu, M., Kasibhatla, P. S., Morton, D. C., DeFries, R. S., Jin, Y., and van Leeuwen, T. T.: Global fire emissions and the contribution of deforestation, savanna, forest, agricultural, and peat fires (1997–2009),

Atmos. Chem. Phys., 10, 11707–11735, doi:10.5194/acp-10-11707-2010, 2010.

Wilson, C., Chipperfield, M. P., Gloor, M., and Chevallier, F.: Development of a variational flux inversion system (INVICAT v1.0) using the TOMCAT chemical transport model, Geosci. Model Dev., 7, 2485–2500, doi:10.5194/gmd-7-2485-2014, 2014.

WDCGG: WMO World Data Centre for Greenhouse Gases, Japan Meteorological Agency, Tokyo, available at: http://ds.data.jma.go.jp/gmd/wdcgg/introduction.html, 2015.

Yokota, T., Yoshida, Y., Eguchi, N., Ota, Y., Tanaka, T., Watanabe, H., and Maksyutov, S.: Global concentrations of $CO_2$ and $CH_4$ retrieved from GOSAT: First preliminary results, SOLA, 5, 160–163, doi:10.2151/sola.2009-041, 2009.

**Table 1.** The coupled model setups analyzed in this study.

| Case | Resolution, ° | | Flux combination |
|---|---|---|---|
| | NIES TM | FLEXPART | |
| Cs-1 | 10.0 | 1.0 | VISIT + CDIAC + OTTM |
| Cs-2 | 2.50 | 1.0 | VISIT + CDIAC + OTTM |
| Cs-3 | 1.25 | 1.0 | VISIT + CDIAC + OTTM |

**Table 2.** WDCGG continuous observation sites.

| # | Identifying code | Location | Lat., ° | Lon.,° | Height, m |
|---|---|---|---|---|---|
| 1 | ALT | Alert, Canada | 82.45 | -62.52 | 210 |
| 2 | AMS | Amsterdam Island, France | -37.8 | 77.53 | 55 |
| 3 | AMY | Anmyeon-do, Korea | 36.53 | 126.32 | 47 |
| 4 | BRW | Barrow, USA | 71.32 | -156.6 | 11 |
| 5 | CMN | Monte Cimone, Italy | 44.18 | 10.7 | 2165 |
| 6 | CPT | Cape Point, South Africa | -34.35 | 18.48 | 230 |
| 7 | HUN | Hegyhatsal, Hungary | 46.95 | 16.65 | 248 |
| 8 | IZO | Izana, Spain | 28.3 | -16.5 | 2367 |
| 9 | JBN | Jubany, Argentina | -62.23 | -58.67 | 15 |
| 10 | MHD | Mace Head, Ireland | 53.33 | -9.9 | 8 |
| 11 | MLO | Mauna Loa, USA | 19.54 | -155.58 | 3397 |
| 12 | MNM | Minamitorishima, Japan | 24.28 | 153.98 | 8 |
| 13 | PAL | Pallas-Sammaltunturi, Finland | 67.97 | 24.12 | 560 |
| 14 | PRS | Plateau Rosa, Italy | 45.93 | 7.7 | 3480 |
| 15 | PUY | Puy de Dome, France | 45.77 | 2.97 | 1465 |
| 16 | SSL | Schauinsland, Germany | 47.92 | 7.92 | 1205 |
| 17 | WSA | Sable Island, Canada | 43.93 | -60.02 | 5 |
| 18 | YON | Yonagunijima, Japan | 24.47 | 123.02 | 30 |
| 19 | ZEP | Zeppelinfjellet, Norway | 78.9 | 11.88 | 475 |

**~~Table 2.~~Table 3.** Tower network sites in Siberia (JR-STATION).

| # | Identifying code | Location | ~~Latitude~~Lat., ° | ~~Longitude~~Lon., ° | ~~Sampling height (m)~~Height, m |
|---|---|---|---|---|---|
| 1 | DEM | Demyanskoe | 59°~~47′29″~~.79 | 70°~~52′16″~~.87 | 63 |
| 2 | IGR | Igrim | 63°~~11′25″~~.19 | 64°~~24′56″~~.42 | 47 |
| 3 | KRS | Karasevoe | 58°~~14′44″~~.25 | 82°~~25′28″~~.42 | 67 |
| 4 | NOY | Noyabrsk | 63°~~25′45″~~.43 | 75°~~46′48″~~.78 | 43 |
| | ~~SVV~~ | ~~Savvushka~~ | ~~51°19′30″~~ | ~~82°07′40″~~ | ~~52~~ |
| 5 | VGN | Vaganovo | 54°~~29′50″~~.50 | 62°~~19′29″~~.32 | 85 |
| 6 | YAK | Yakutsk | 62°~~05′19″~~.09 | 129°~~21′21″~~.36 | 77 |

~~Information on~~

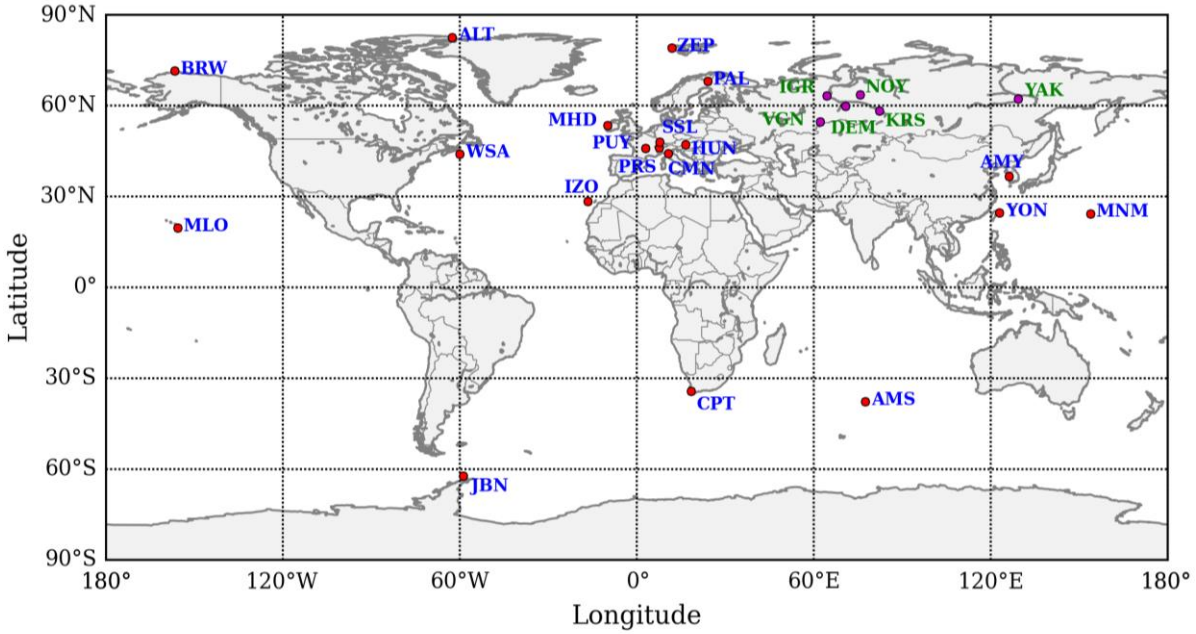


**Fig. 1.** Map showing the location of the 19 WDCGG sites (red dots, blue labels) and 6 tower network sites in Siberia (magenta dots, green labels) for which we have performed comparison using forward GELCA simulation.

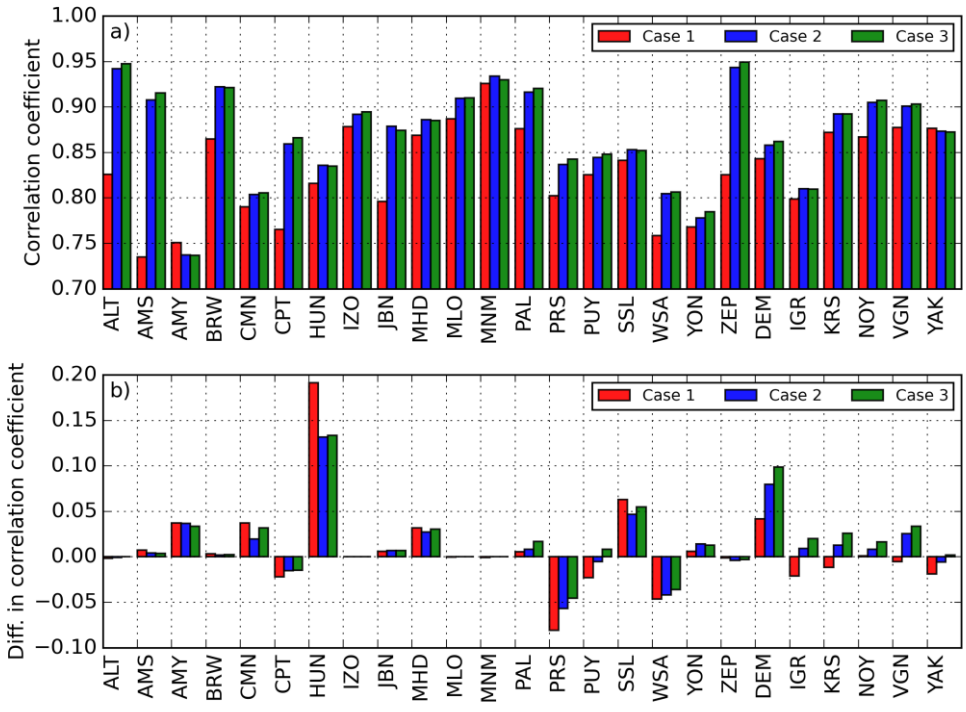

**~~Table 3.~~Fig. 2.** a) Correlation coefficients between the $CO_2$ concentrations simulated with the coupled model and those observed, b) difference in correlation coefficients~~, mean bias, and standard deviations between simulations using the coupled (~~ due to the application of the Lagrangian component (positive values mean the results of the coupled model are better than those of the Eulerian model alone) ~~model and observations.~~ at the selected WDCGG and JR-STATION locations for 2009-2010.

| | | ~~Cs-1~~ | | | ~~Cs-2~~ | | | ~~Cs-3~~ | | |
|---|---|---|---|---|---|---|---|---|---|---|
| ~~Site~~ | ~~# of obs.~~ | ~~Correlation coefficient~~ | ~~Mean bias, ppm~~ | ~~STD, ppm~~ | ~~Correlation coefficient~~ | ~~Mean bias, ppm~~ | ~~STD, ppm~~ | ~~Correlation coefficient~~ | ~~Mean bias, ppm~~ | ~~STD, ppm~~ |
| ~~DEM~~ | ~~304~~ | ~~0.85 (0.85)~~ | ~~2.92 (3.68)~~ | ~~4.19 (4.37)~~ | ~~0.86 (0.84)~~ | ~~1.27 (2.03)~~ | ~~4.01 (4.37)~~ | ~~0.87 (0.84)~~ | ~~0.69 (1.45)~~ | ~~4.02 (4.27)~~ |
| ~~IGR~~ | ~~576~~ | ~~0.84 (0.87)~~ | ~~2.08 (2.72)~~ | ~~6.51 (7.27)~~ | ~~0.86 (0.86)~~ | ~~1.01 (1.66)~~ | ~~6.2 (7.13)~~ | ~~0.86 (0.85)~~ | ~~0.58 (1.23)~~ | ~~6.16 (7.07)~~ |
| ~~KRS~~ | ~~509~~ | ~~0.88 (0.9)~~ | ~~1.04 (1.44)~~ | ~~5.57 (6.66)~~ | ~~0.90 (0.91)~~ | ~~-0.05 (0.36)~~ | ~~4.92 (5.95)~~ | ~~0.91 (0.91)~~ | ~~-0.63 (-0.23)~~ | ~~4.79 (5.79)~~ |
| ~~NOY~~ | ~~382~~ | ~~0.86 (0.87)~~ | ~~1.48 (2.04)~~ | ~~5.24 (5.72)~~ | ~~0.90 (0.9)~~ | ~~0.07 (0.63)~~ | ~~4.51 (5.08)~~ | ~~0.91 (0.91)~~ | ~~-0.45 (0.12)~~ | ~~4.37 (4.9)~~ |
| ~~SVV~~ | ~~394~~ | ~~0.89 (0.88)~~ | ~~0.44 (0.16)~~ | ~~6.56 (7.62)~~ | ~~0.91 (0.88)~~ | ~~0.34 (0.06)~~ | ~~5.72 (6.74)~~ | ~~0.90 (0.88)~~ | ~~0.01 (-0.27)~~ | ~~5.6 (6.6)~~ |
| ~~VGN~~ | ~~609~~ | ~~0.88 (0.9)~~ | ~~1.49 (1.69)~~ | ~~5.04 (5.74)~~ | ~~0.91 (0.9)~~ | ~~0.62 (0.82)~~ | ~~4.36 (5.13)~~ | ~~0.91 (0.9)~~ | ~~0.25 (0.45)~~ | ~~4.23 (5.01)~~ |
| ~~YAK~~ | ~~405~~ | ~~0.84 (0.87)~~ | ~~1.22 (2.44)~~ | ~~5.37 (5.12)~~ | ~~0.86 (0.87)~~ | ~~-0.28 (0.94~~ | ~~5.68 (4.64)~~ | ~~0.85 (0.86)~~ | ~~-0.81 (0.42)~~ | ~~5.95 (4.74)~~ |
| ~~Average~~ | | ~~0.86 (0.88)~~ | ~~1.52 (2.02)~~ | ~~5.50 (6.07)~~ | ~~0.89 (0.88)~~ | ~~0.43 (0.93)~~ | ~~5.06 (5.58)~~ | ~~0.89 (0.88)~~ | ~~-0.05 (0.45)~~ | ~~5.02 (5.48)~~ |

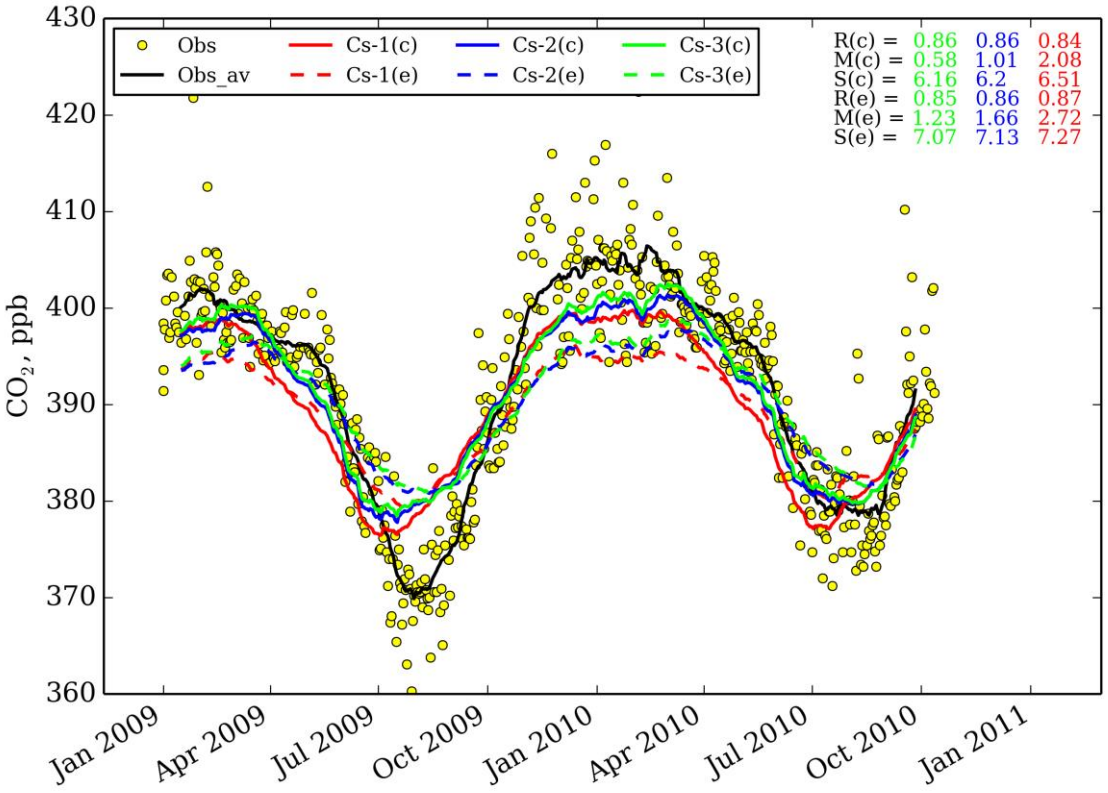
Obs
Obs_av
Cs-1(c)
Cs-1(e)
Cs-2(c)
Cs-2(e)
Cs-3(c)
Cs-3(e)
R(c) = 0.86 0.86 0.84
M(c) = 0.58 1.01 2.08
S(c) = 6.16 6.2 6.51
R(e) = 0.85 0.86 0.87
M(e) = 1.23 1.66 2.72
S(e) = 7.07 7.13 7.27
$CO_2$, ppb
430
420
410
400
390
380
370
360
Jan 2009
Apr 2009
Jul 2009
Oct 2009
Jan 2010
Apr 2010
Jul 2010
Oct 2010
Jan 2011

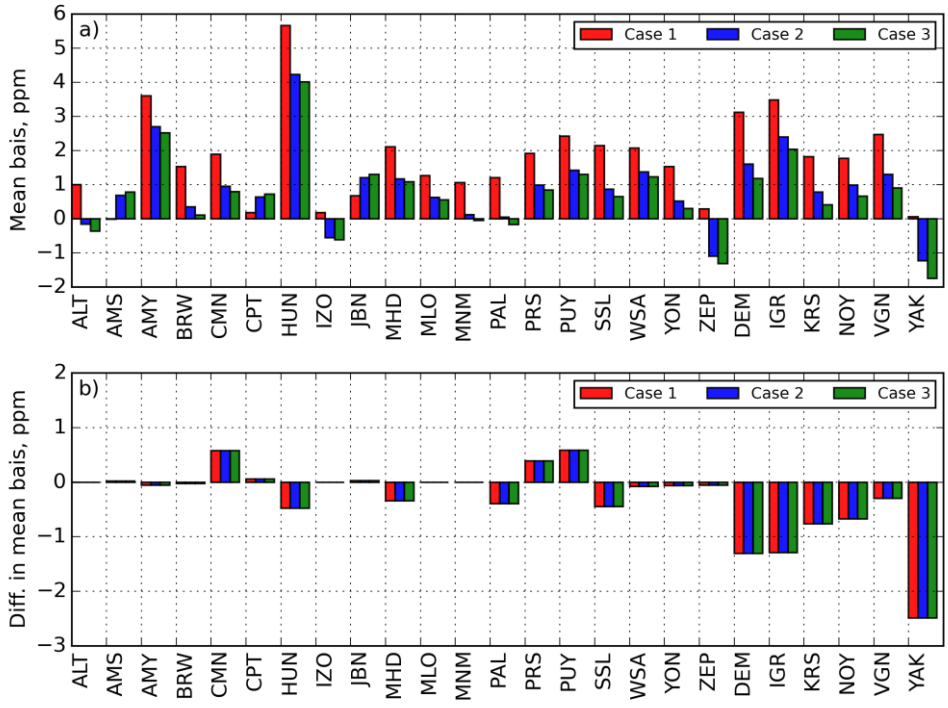
a)
Case 1
Case 2
Case 3
Mean bais, ppm
b)
Diff. in mean bais, ppm
ALT
AMS
AMY
BRW
CMN
CPT
HUN
IZO
JBN
MHD
MLO
MNM
PAL
PRS
PUY
SSL
WSA
YON
ZEP
DEM
IGR
KRS
NOY
VGN
YAK

**Fig. 3.** a) Mean bias for the CO2 concentrations simulated with the coupled model, b) difference in mean bias due to the application of the Lagrangian component (for positive bias – the most usual case – negative values mean the results of the coupled model are better than those of the Eulerian model alone) at the selected WDCGG and JR-STATION locations for 2009-2010.

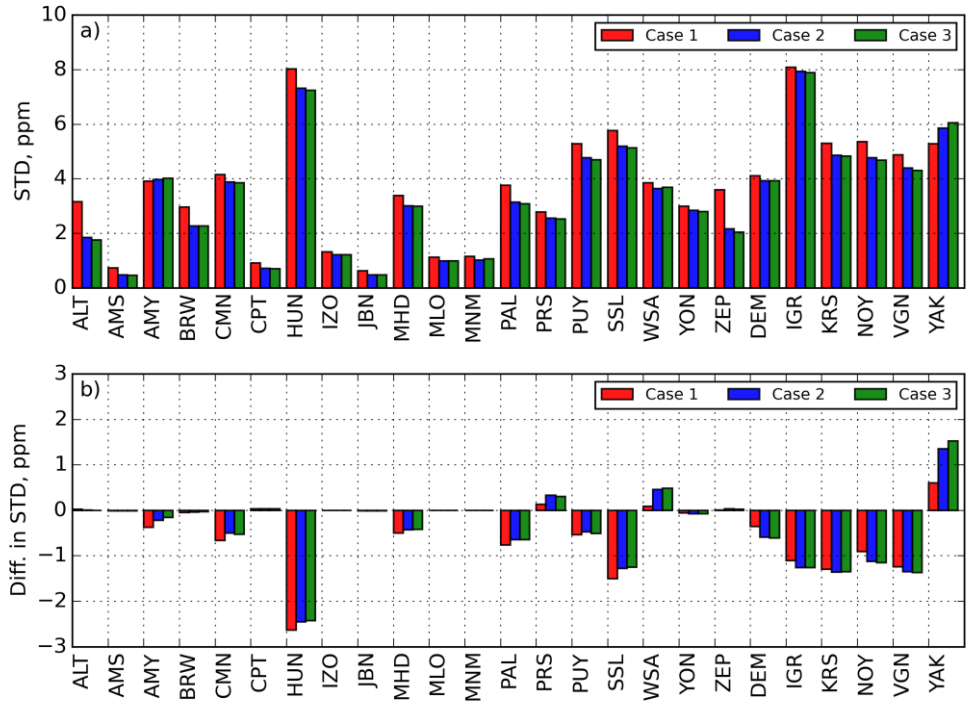


**Fig. 4.** a) Standard deviation (STD) for the $CO_2$ concentration model-observation mismatch when using the coupled model, b) difference in STD due to the application of Lagrangian component (negative values mean the results of the coupled model are better than of the Eulerian model alone) at the selected WDCGG and JR-STATION locations for 2009-2010.

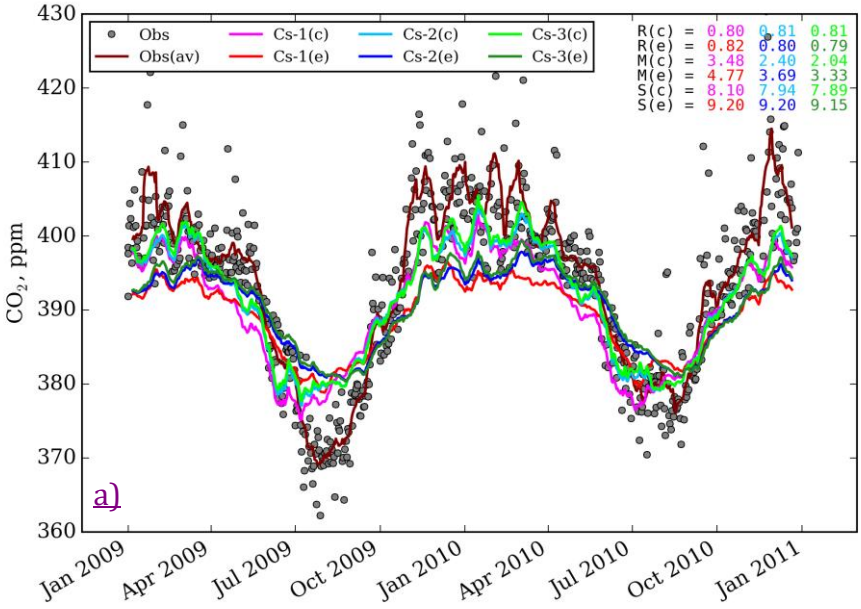


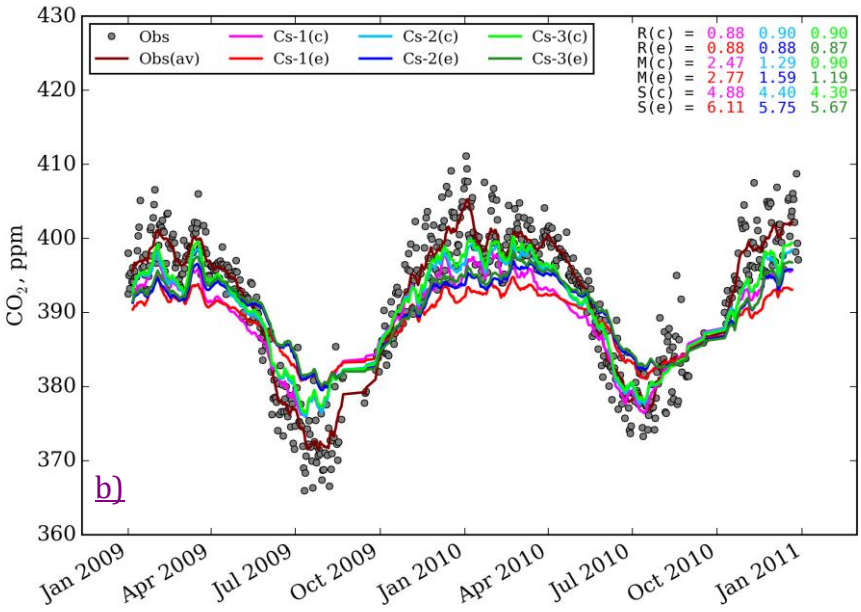


**~~Fig. 1.~~Fig. 5.** $CO_2$ mixing ratios observed at a) the Igrim ~~tower~~and b) Vaganovo towers, and simulated using the coupled ~~("~~("c~~"; solid line~~) and Eulerian-only ~~("~~("e~~"; dotted line~~) models using the ~~model~~ setups from Table 1 for 2009–2010. Symbols show individual observations; lines depict ~~the moving average.~~two-weeks running averages. Here, ~~r, s, m~~R, S and M mean the Pearson correlation, standard deviation and mean bias ~~correspondently~~respectively.

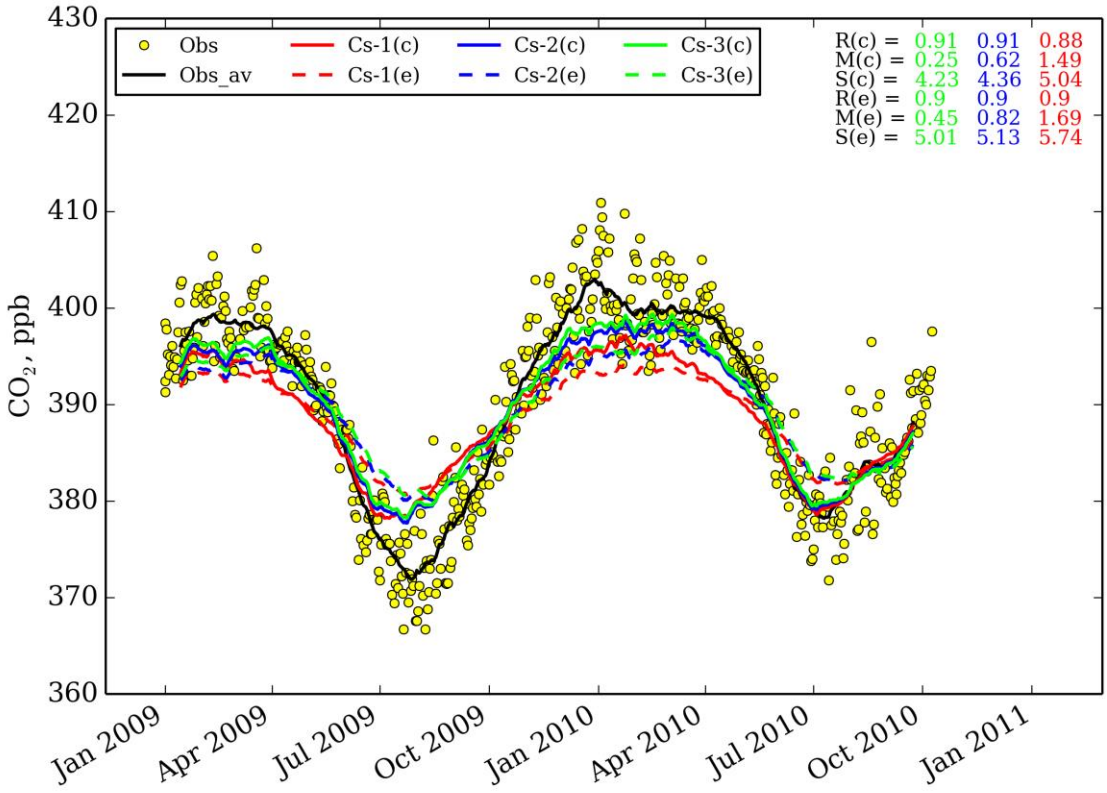


**~~Fig. 2.~~** ~~As for Fig 2, but for the Vaganovo tower.~~

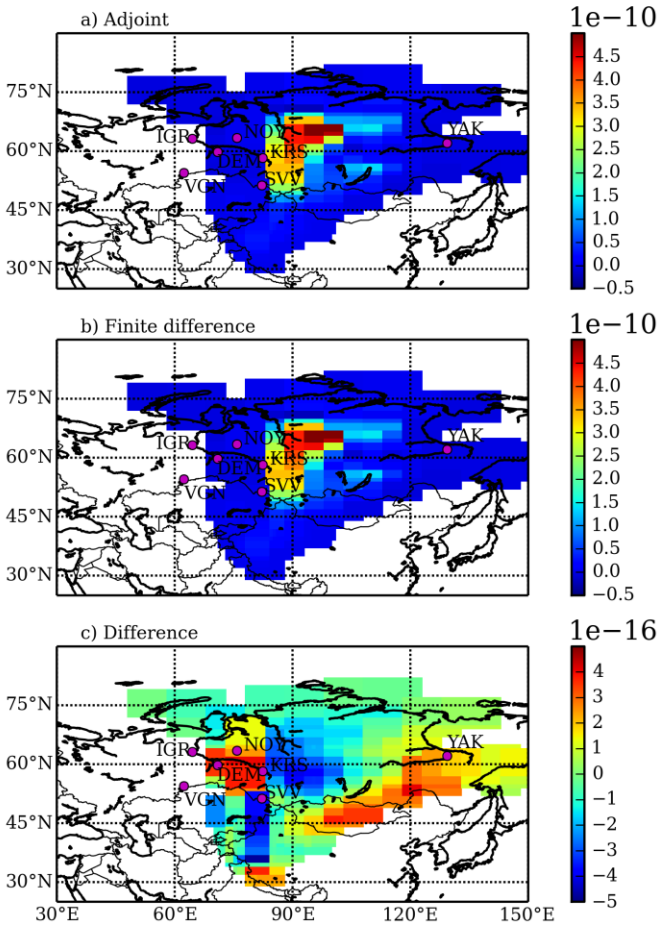
a) Adjoint
1e−10
4.5
4.0
3.5
3.0
2.5
2.0
1.5
1.0
0.5
0.0
−0.5
b) Finite difference
1e−10
c) Difference
1e−16
4
3
2
1
0
−1
−2
−3
−4
−5
75°N
60°N
45°N
30°N
30°E
60°E
90°E
120°E
150°E
IGR
NOY
KRS
DEM
SVV
VGN
YAK

1

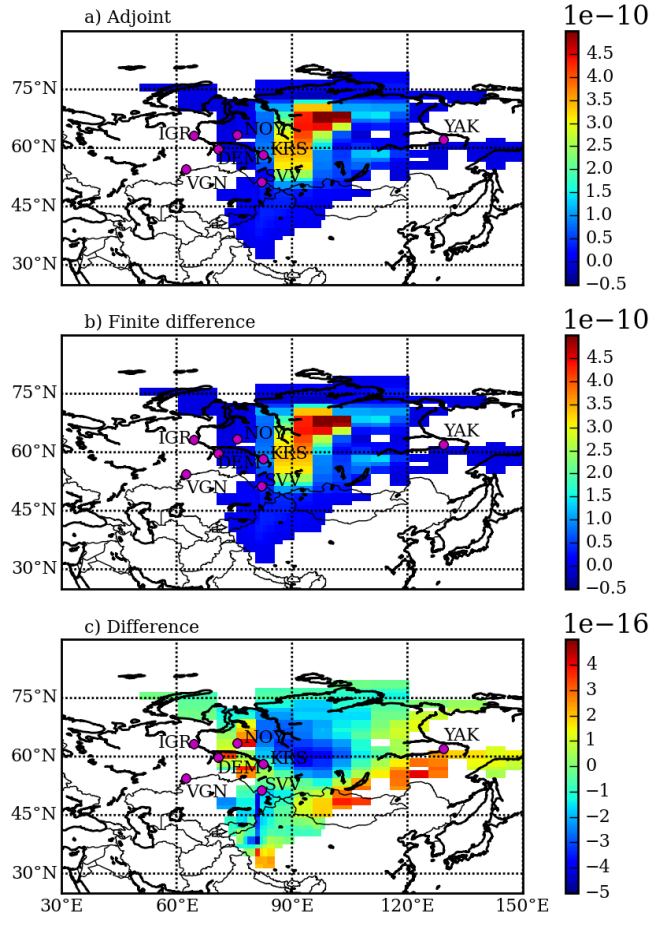
a) Adjoint
1e−10
4.5
4.0
3.5
3.0
2.5
2.0
1.5
1.0
0.5
0.0
−0.5
b) Finite difference
1e−10
c) Difference
1e−16
4
3
2
1
0
−1
−2
−3
−4
−5
75°N
60°N
45°N
30°N
30°E
60°E
90°E
120°E
150°E
IGR
NOY
KRS
DEM
SVV
VGN
YAK

2

~~Fig. 3.~~Fig. 6. Comparison of sensitivities of $CO_2$ concentrations (ppm/(μmol/$m^2$s)) for test 1: (a) sensitivity calculated considering only the Eulerian adjoint model at a resolution of 2.5°, (b) the same sensitivity calculated directly from NIES forward runs using the one-sided numerical finite difference method with perturbations of $\varepsilon$, and c) the relative difference between derived adjoint and the numerical finite difference gradients. Magenta dots with labels depicts the locations and names of the Siberian ~~observations~~observation towers.

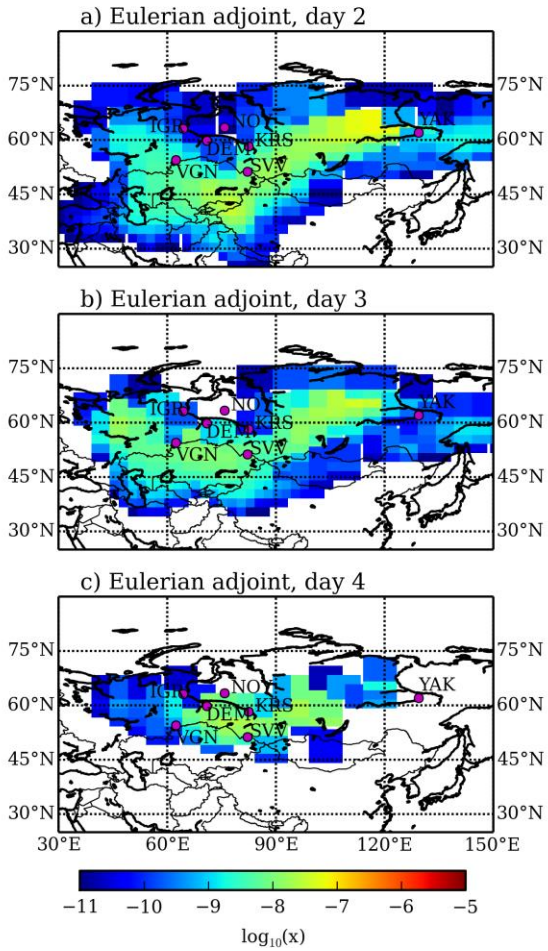


Sensitivities

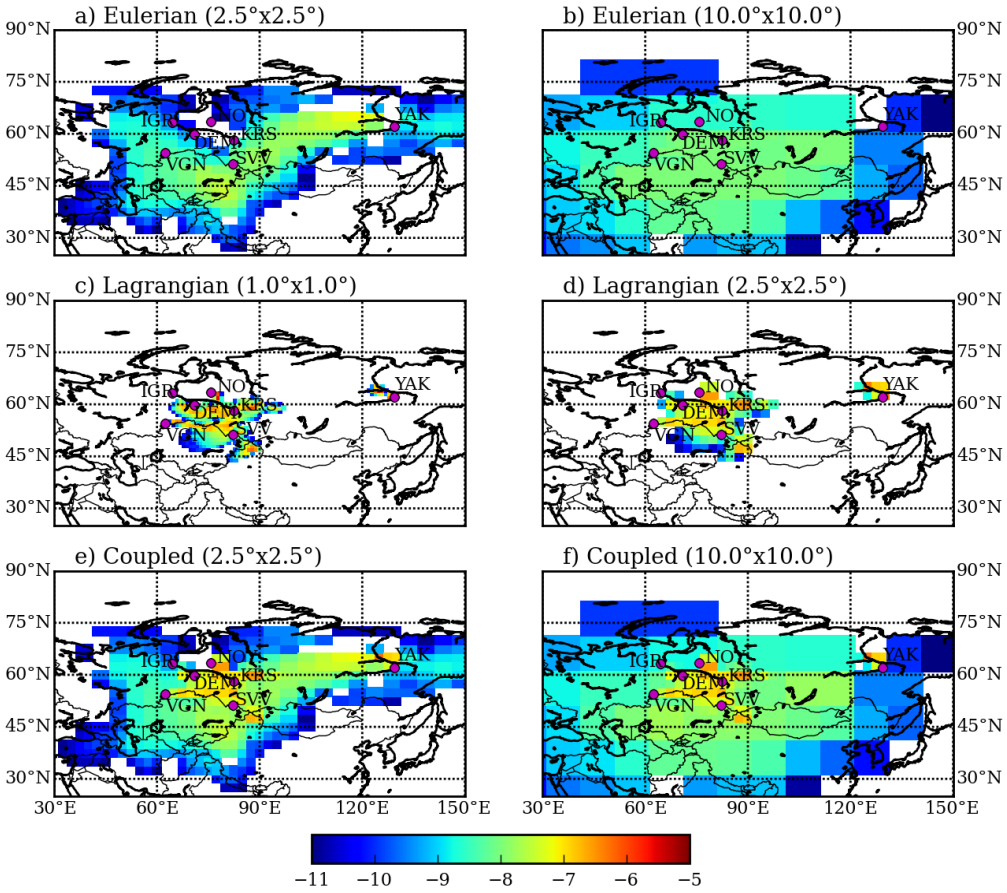


**~~Fig. 4.~~** Comparison of sensitivities of $CO_2$ concentrations ~~([~~[ppm/(µmol/$m^2$s)~~) with respect to concentrations in adjacent cells, considering only~~)] at day 2 (see Sect. 5.2.2) calculated using: a) the Eulerian adjoint ~~model at~~with a resolution of 2.5~~°~~.

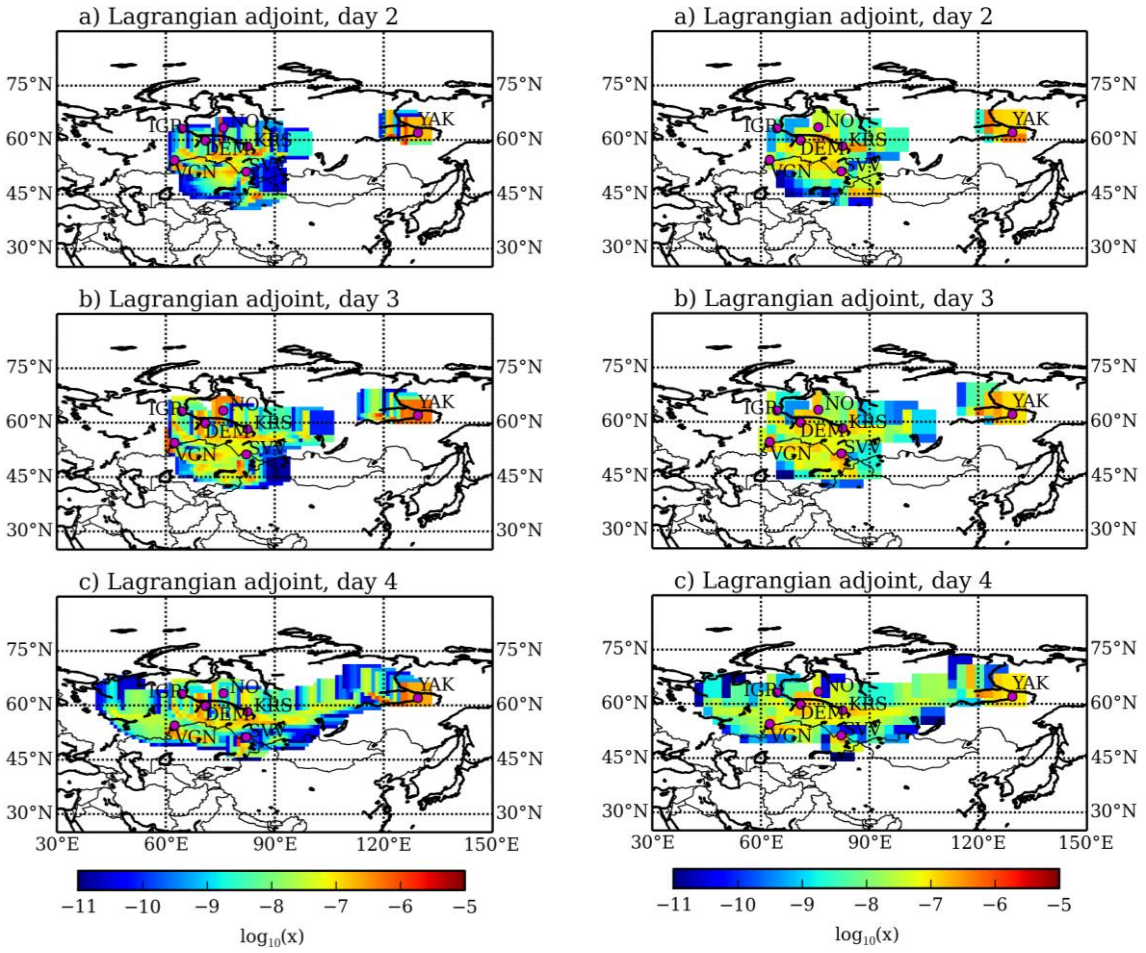


**~~Fig. 5.~~** ~~Same as Fig.4, but considering only~~°, b) the Eulerian adjoint with a resolution of 10.0°, c) the Lagrangian ~~adjoint~~ model~~. The left panels show results~~ on the native model grid with a resolution of 1.0°, ~~while the right panels show the results~~ d) as for c), but aggregated on the grid ~~at~~with a resolution of 2.5~~°.~~

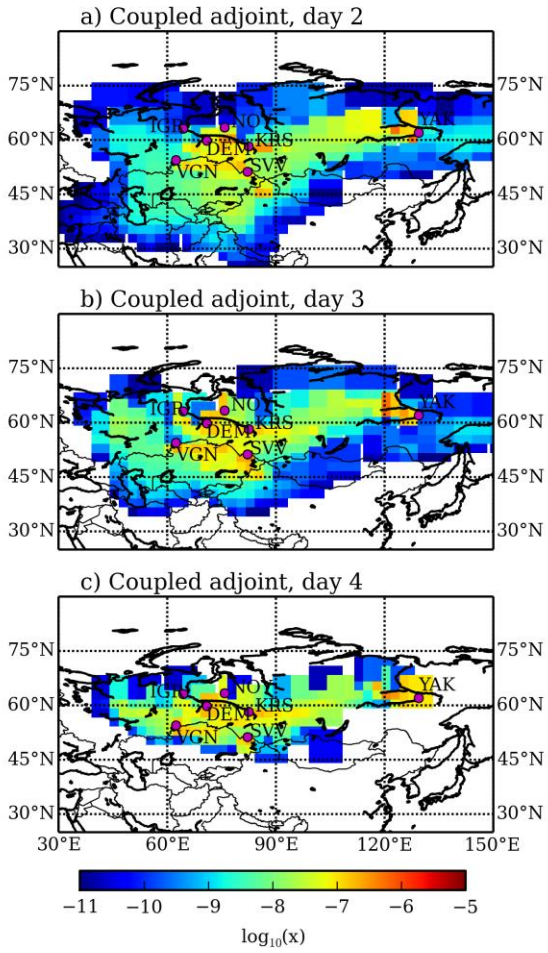


**~~Fig. 6.~~** ~~Same as Fig.4, but considering~~°, e) the coupled adjoint model~~. Results~~; results from the Lagrangian adjoint model were aggregated on the grid ~~of NIES TM at~~with a resolution of 2.5~~°.~~

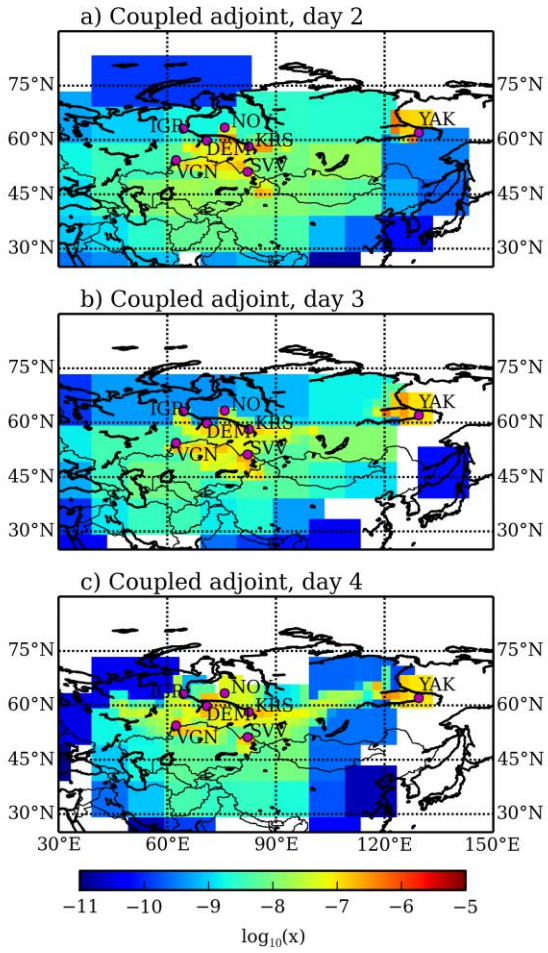


**Fig. 7.** ~~As~~°, f) as for ~~Fig. 6,~~e), but ~~results from~~the resolution of the Eulerian adjoint model ~~were aggregated on~~was 10.0°. Note the ~~grid at a resolution of 10.0°.~~logarithmic color scale for the plots.

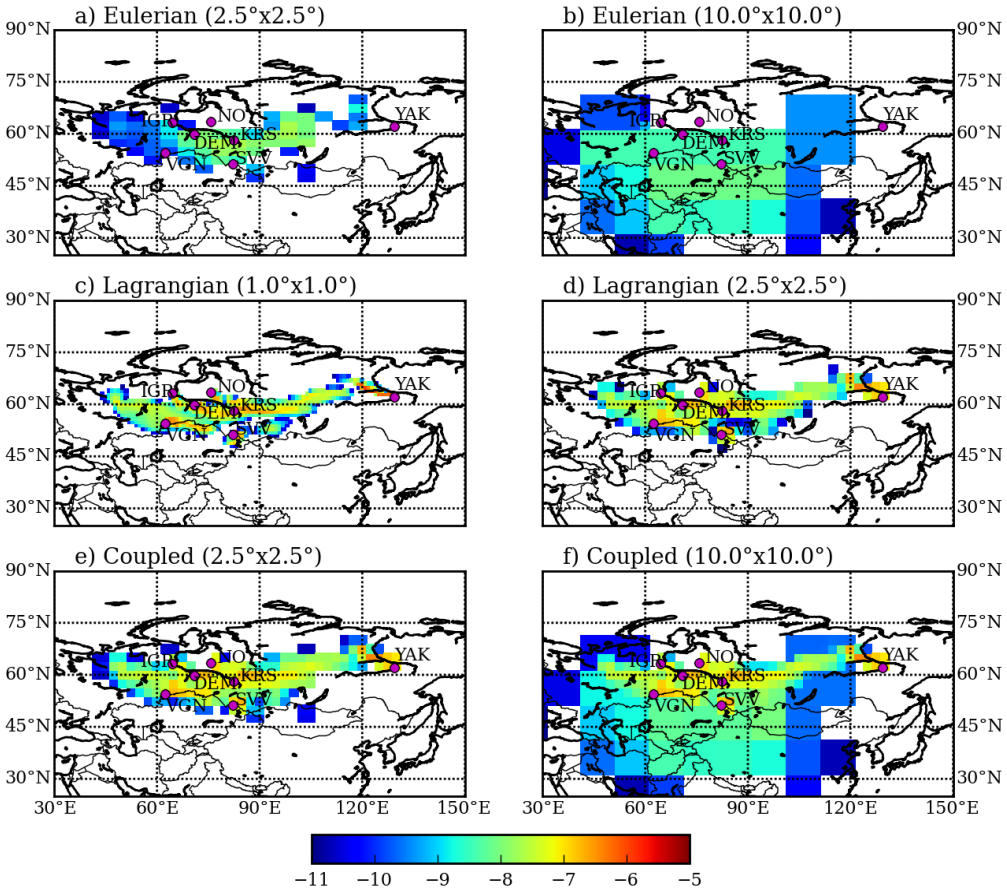


**Fig. 8.** As for Fig. 7, but for day 4.